Sitzungsberichte der Heidelberger Akademie der Wissenschaften
Mathematisch-naturwissenschaftliche Klasse

Die Jahrgänge bis 1921 einschließlich erschienen im Verlag von Carl Winter, Universitätsbuchhandlung in Heidelberg, die Jahrgänge 1922–1933 im Verlag Walter de Gruyter & Co. in Berlin, die Jahrgänge 1934–1944 bei der Weißschen Universitätsbuchhandlung in Heidelberg. 1945, 1946 und 1947 sind keine Sitzungsberichte erschienen.

Ab Jahrgang 1948 erscheinen die „Sitzungsberichte" im Springer-Verlag.

Inhalt des Jahrgangs 1958:

1. W. Rauh. Beitrag zur Kenntnis der peruanischen Kakteenvegetation. (vergriffen).
2. W. Kuhn. Erzeugung mechanischer aus chemischer Energie durch homogene sowie durch quergestreifte synthetische Fäden. (vergriffen).

Inhalt des Jahrgangs 1959:

1. W. Rauh und H. Falk. Stylites E. Amstutz, eine neue Isoëtacee aus den Hochanden Perus. 1. Teil. DM 30.40.
2. W. Rauh und H. Falk. Stylites E. Amstutz, eine neue Isoëtacee aus den Hochanden Perus. 2. Teil. DM 42.90.
3. H. A. Weidenmüller. Eine allgemeine Formulierung der Theorie der Oberflächenreaktionen mit Anwendung auf die Winkelverteilung bei Strippingreaktionen. DM 12.00.
4. M. Ehlich und M. Müller. Über die Differentialgleichungen der bimolekularen Reaktion 2. Ordnung. (vergriffen).
5. Vorträge und Diskussionen beim Kolloquium über Bildwandler und Bildspeicherröhren. Herausgegeben von H. Siedentopf. DM 21.00.
6. H. J. Mang. Zur Theorie des α-Zerfalls. DM 12.00.

Inhalt des Jahrgangs 1960/61:

1. R. Berger. Über verschiedene Differentenbegriffe. (vergriffen).
2. P. Swings. Problems of Astronomical Spectroscopy. (vergriffen).
3. H. Kopfermann. Über optisches Pumpen an Gasen. (vergriffen).
4. F. Kasch. Projektive Frobenius-Erweiterungen. DM (vergriffen).
5. J. Petzold. Theorie des Mößbauer-Effektes. DM 17.90.
6. O. Renner. William Bateson und Carl Correns. DM 12.00.
7. W. Rauh. Weitere Untersuchungen an Didiereaceen. 1. Teil. DM 56.90.

Inhalt des Jahrgangs 1962/64:

1. E. Rodenwaldt und H. Lehmann. Die antiken Emissare von Cosa-Ansedonia, ein Beitrag zur Frage der Entwässerung der Maremmen in etruskischer Zeit. DM 12.00.
2. Symposium über Automation und Digitalisierung in der Astronomischen Meßtechnik. Herausgegeben von H. Siedentopf. (vergriffen).
3. W. Jehne. Die Struktur der symplektischen Gruppe über lokalen und dedekindschen Ringen. (vergriffen).
4. W. Doerr. Gangarten der Arteriosklerose. (vergriffen).
5. J. Kuprianoff. Probleme der Strahlenkonservierung von Lebensmitteln. (vergriffen).
6. P. Čolak-Antič. Dreidimensionale Instabilitätserscheinungen des laminarturbulenten Umschlages bei freier Konvektion längs einer vertikalen geheizten Platte. DM 18.70.

Inhalt des Jahrgangs 1965:

1. S. E. Kuss. Revision der europäischen Amphicyoninae (Canidae, Carnivora, Mam.) ausschließlich der voroberstampischen Formen. DM 50.40.
2. E. Kauker. Globale Verbreitung des Milzbrandes um 1960. DM 12.00.
3. W. Rauh und H. F. Schölch. Weitere Untersuchungen an Didieraceen. 2. Teil. DM 91.00.
4. W. Felscher. Adjungierte Funktoren und primitive Klassen. (vergriffen).

Sitzungsberichte der Heidelberger Akademie der Wissenschaften
Mathematisch-naturwissenschaftliche Klasse,
Jahrgang 1976, 3. Abhandlung

M. Steinhausen G. A. Tanner

Microcirculation and Tubular Urine Flow in the Mammalian Kidney Cortex (in vivo Microscopy)

With 12 Figures

(Submitted to the Academy Session of April 24, 1976)

Springer-Verlag Berlin Heidelberg New York 1976

Professor Dr. Michael Steinhausen
I. Physiologisches Institut der Universität, Im Neuenheimer Feld 326
6900 Heidelberg (W-Germany)

George A. Tanner, Ph. D.
Associate Professor of Physiology Department of Physiology,
Indiana University School of Medicine, 1100 West Michigan Street
Indianapolis, Indiana 46202 (U.S.A)

(Gastprofessor I. Physiologisches Institut, Universität Heidelberg,
Juli 1974 — Juni 1975)

ISBN-13: 978-3-540-07819-7 e-ISBN-13: 978-3-642-46340-2
DOI: 10.1007/978-3-642-46340-2

Universitätsdruckerei H. Stürtz AG, Würzburg

Microcirculation and Tubular Urine Flow in the Mammalian Kidney Cortex (in vivo Microscopy)*, **

M. Steinhausen and G. A. Tanner

I. Physiologisches Institut der Universität Heidelberg

Table of Contents

---

* Dedicated to Hans Schaefer, Dr. med., em. Professor of Physiology, University of Heidelberg on his 70th anniversary (August 13th, 1976).

** The original research was supported by the Deutsche Forschungsgemeinschaft (SFB 90). We thank Dr. G. Giebisch for helpful suggestions.

I. Introduction

The surface of the kidney presents a unique opportunity to study fundamental processes in the living animal. Here blood vessels and kidney tubules are accessible to direct microscopic observation. This situation has been used to elucidate kidney functions under normal and pathological conditions.

A number of observations on function in the intact kidney can be made through the microscope. We can observe the flow of blood in the renal microcirculation on the cortical surface. We can identify proximal and distal tubules, and measure their widths. We can follow the flow of tubular fluid with the use of dyes. We can watch fluid reabsorption in tubular segments isolated by oil droplets. With photography, these observations can be recorded and quantitated. In this monograph, we will survey the methods and results of in vivo microscopy of the kidney cortex. We will consider the advantages and limitations of these methods, and discuss their contributions to our understanding of kidney physiology.

A general discussion of kidney function may be found in Ref. [127]. The reader is also referred to several recent reviews and books on the kidney [28, 41, 43, 66, 72a, 84, 95, 120, 128, 136, 140, 194, 203, 204, 210, 216].

General Techniques

The study of mammalian kidney function by in vivo microscopy is more than 60 years old. Ghiron [64] was the first to observe the functioning mouse kidney through the microscope. Edwards and Marshall [46] presented the first drawing of the renal surface of the rat as seen through the incident light microscope. They noticed that proximal tubule lumens of the rat kidney dilated during a sulfate diuresis. Walker and Oliver [199] were first to apply micropuncture techniques to the mammalian kidney.

The kidney is routinely exposed for visual observation in micropuncture studies. Most observations of renal cortical function in vivo have been made in the rat. However, observations have also been made in other mammals, e.g. mouse, guinea pig, Psammomys, hamster, dog, cat, and monkey. The experimental approach is basically similar in all species, but in the larger animals, the kidney must be decapsulated in order to see the tubules.

The kidney is surgically exposed in the anesthetized animal. It is usually dissected free from perirenal fat and is supported in a spoon-shaped holder to minimize disturbing respiratory movements. A notch in the holder provides space for the blood vessels and ureter which enter and leave the kidney at the hilus. The reader is referred to the monograph by Windhager [215] and to the article by Gottschalk [127] for discussion of micropuncture techniques.

Certain difficulties inherent in studies of renal function by in vivo microscopy must be kept in mind. First, renal tubules and blood vessels are tightly enmeshed in a complex structure. Second, blood and tubular urine flow patterns within the kidney differ from those visible on the surface. Third, interference with the normally extremely high blood flow through the renal cortex leads to changes in function and structure. Finally, observations are made on anesthetized animals, which have often been subjected to extensive surgery[1]. Because of these problems, we must be cautious in applying results from in vivo microscopy to whole kidney function in the normal animal.

Stereomicroscopes are most often used for observing the kidney in micropuncture studies. The magnification with these microscopes is usually limited to 100–200 powers. Greenough objectives, used in the Leitz stereomicroscopes, are recommended because they provide high magnification and high resolution. We have also used a large Zeiss double-headed operating microscope (objective f=50 mm) with a zoom lens. This microscope, however, tends to swing about the microscope stand, so additional support on the operating table is necessary. Photomicrography with stereomicroscopes is not optimal, because only strongly contrasted phenomena (e.g. Sudan black stained castor oil injected into a tubule) can be visualized. The weakly contrasting surface of the kidney is best photographed with incident light darkfield illumination using Leitz Ultropak objectives. For high magnification incident light fluorescence microscopy, immersion objectives with a combination of illumination and observation beams (e.g. Leitz Fluopak system) are suitable. Microcinematography can also be done [163, 167, 170, 178, 191]. For high frequency microcinematography [170], a high light intensity is needed, and heat absorbing filters are required to avoid damaging the kidney.

Histological techniques are a valuable supplement to in vivo observations of renal function. Casts of the renal vasculature and tubule system are especially helpful in defining the three-dimensional architecture of the kidney. Figure 1 shows a cast preparation from a fixed and cleared rat kidney. The vascular system was filled with red latex from the renal artery and the renal tubule with white latex by micropuncture of the renal surface. Only the proximal convoluted tubule is filled, and filling of the venous portion of the renal vasculature is lacking. Figure 2 shows a diagrammatic drawing of a superficial cortical nephron based on such cast preparations. The renal microvasculature of such a nephron includes: afferent arteriole (vas afferens), glomerulus, efferent arteriole (vas efferens), welling or source point, peritubular capillary network, and venule. The renal corpuscle (Malpighian body) consists of the glomerular capillary tuft surrounded by

1 We have recently developed a new kidney chamber which permits microscopic observation of the kidney surface in the unanesthetized rat ([174a]; see also p. 34).

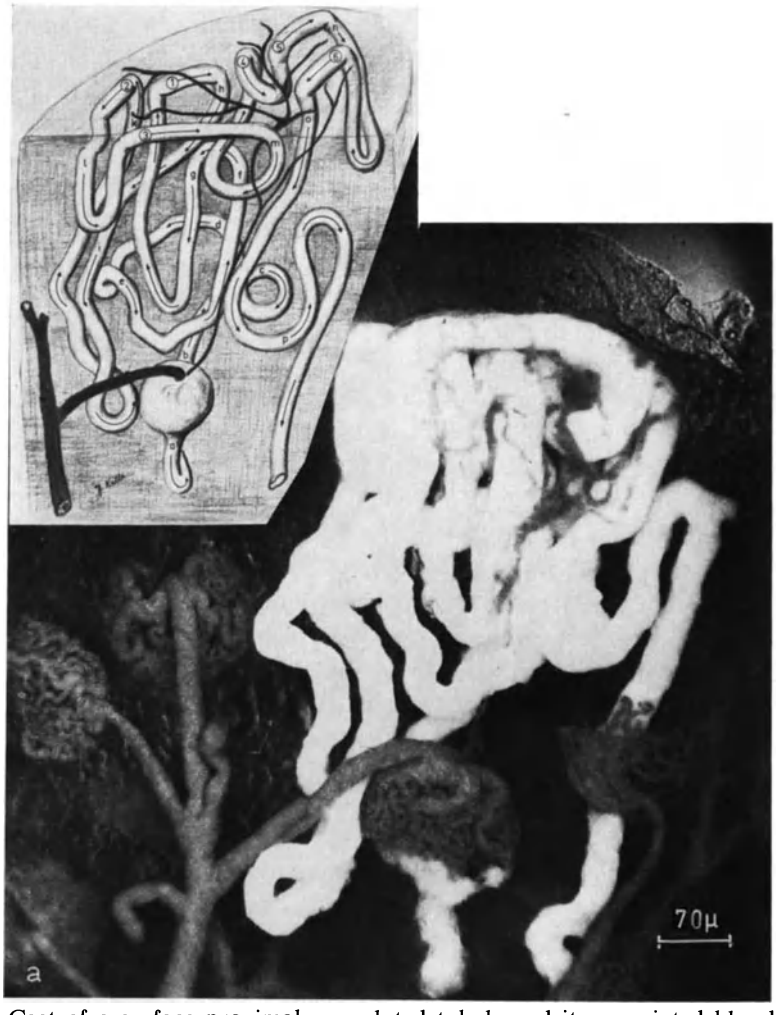

Fig. 1. Cast of a surface proximal convoluted tubule and its associated blood supply. The kidney was made transparent by treating it for a few seconds with concentrated KOH. The inset shows a three dimensional depiction of a proximal tubule. The tubular fluid flow direction is shown by arrows and is numbered numerically. The letters mark the sequence of proximal tubular loops, starting from the glomerulus. The vas afferens is dilatated for technical reasons (cf. Table 16). (From Steinhausen *et al.* [173])

the blind end of the proximal tubule (Bowman's capsule). An ultrafiltrate of blood plasma is formed by the glomerulus and flows down the tubule, where it is changed into urine. The tubule consists of proximal convoluted tubule, loop of Henle, and distal convoluted tubule. Distal convoluted tubules join via connecting tubules to form the collecting tubules.

In vivo observation of the kidney cortex surface provides a limited view of renal structures. Glomeruli are usually absent from the surface of the mam-

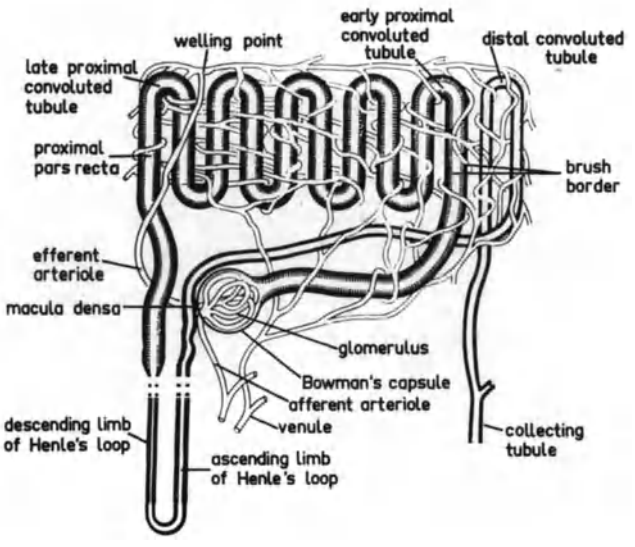

Fig. 2. Schematic drawing of a superficial nephron and its blood supply. (From Steinhausen [169])

malian kidney. Occasional superficial glomeruli are encountered in the guinea pig [199], immature mouse [76], rats [160], Munich strain Wistar rat [26, 75, 170] and squirrel monkey [109, 187]. Afferent arterioles have not been observed at the renal surface, and only the branching point of the efferent arteriole (welling point) is visible. Most of the tubule loops on the kidney surface (about 94 % in the rat) belong to proximal convoluted tubules; the rest are distal convoluted tubule loops [160, 199]. An average of 5.2 ± 0.6 SE ($n = 56$) loops of a proximal convoluted tubule are visible on the surface, but this is less than 20 % of the total length of this tubule segment [173]. Loops of Henle and medullary collecting ducts can be visualized only by exposing the renal papilla. Cortical collecting tubules are inaccessible to in vivo observation. Lymph vessels are absent from the superficial cortex in most of the rodent kidneys studied [92]. Despite strenuous efforts, the interstitial space remains as invisible to intravital microscopists as the soul to Virchow.

II. Measurements of Tubular Lumen Diameter

A. General

In the normal intact functioning kidney, the kidney tubule lumens are all open. By contrast, in kidneys fixed for histology, tubule lumens are often collapsed. Lumen collapse reflects continued fluid reabsorption at a time when glomerular filtration has ceased (Fig. 3 [175]). Rapid fixation of kidney tissue is essential to preserve normally open lumens. Fixatives may be ap-

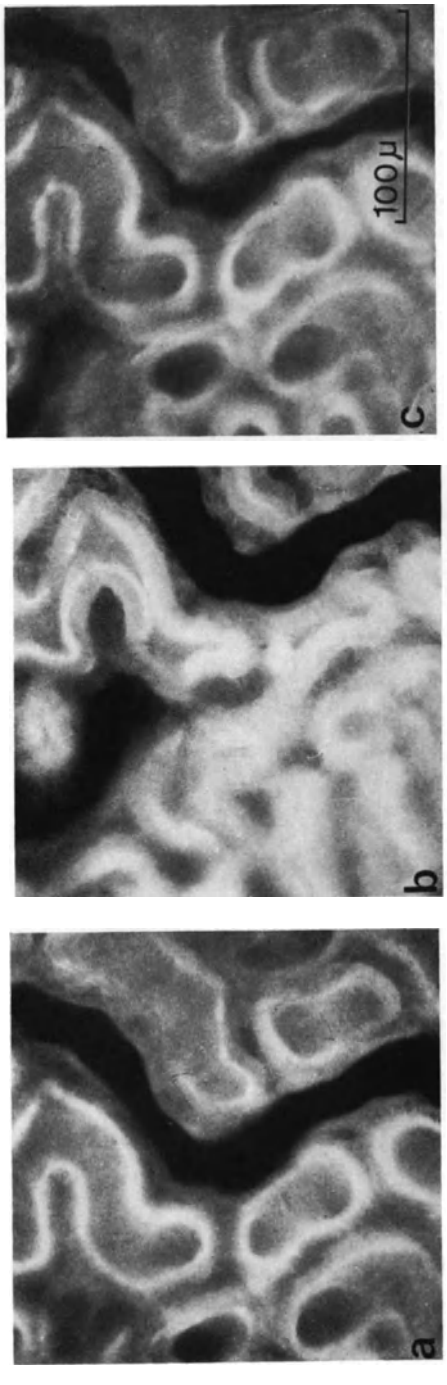

Fig. 3. Effect of temporary occlusion of the aorta on tubule lumen diameters. Lissamine green was injected i.v. for a passage time determination and causes the dark appearance of the distal convoluted tubule lumen in the microphotographs. (a) Before clamping the aorta. (b) 40 sec after clamping the aorta. Note the collapse of the proximal tubule lumens. (c) After release of the clamp on the aorta. Note the filling of proximal tubules and the compression of the distal tubule.
(From Steinhausen et al. [175]

plied intravitally directly on the surface of the kidney [94, 117, 132, 133], by perfusing individual nephrons with fixing fluid [115, 189], or by perfusing the kidneys with fixative solution in vivo [42, 72, 115, 145, 192]. Rapidfreezing of the kidney has also been used [7, 17, 77, 100, 175]. Conclusions about tubular diameters in vivo from fixed tissues must be judged cautiously, because of possible alterations due to insufficiently rapid fixation and changes produced by processing of the tissue for histology.

The most reliable measurements of tubular diameters under different physiological conditions are obtained by in vivo microscopy and photography. Clear, sharp pictures, taken at a high magnification, are needed for accurate measurements; blurred pictures will give unreliable results. The tubules are not constant bore tubes, and wide or narrow portions of the same tubule can be selected. In assessing diameter changes with the incident light microscope, comparison of lumen diameter at the same place under various conditions provides the most reliable data.

The lumen diameter of a tubule is determined by three factors. The first factor is the difference between internal and external hydrostatic pressures. The distending internal hydrostatic pressure in a tubule is determined by a) the rate of fluid delivery (hence the glomerular filtration rate), b) the rate of tubular reabsorption of fluid, and c) the downstream pressure and resistance to fluid flow. The external hydrostatic pressure (the interstitial fluid pressure) acts to oppose distension, and is normally a few mm Hg [129]. The second factor influencing lumen diameter is tubular distensibility. Welling and Grantham [209] studied this in isolated rabbit kidney tubules. They found that the tubular basement membrane determines the overall distensibility of the tubules. The elastic modulus for tubular basement membrane corresponds closely to that of tendon collagen, indicating a considerable toughness. The tubule wall becomes increasingly stiff as it is stretched. The third factor is the amount of tubular cell hydration. Tubular epithelial cell swelling will act to diminish the diameter of the tubule lumen. In experimental acute kidney failure induced by temporary ischemia [31] or by mercury [91], such cell swelling in the proximal pars recta may nearly obliterate the lumen. The resulting increase in flow resistance may contribute significantly to the renal insufficiency.

B. Proximal Tubule Lumen Diameter

Some controversy surrounds the in vivo measurement of proximal lumen diameter. We believe that the "white zone" which is brightly illuminated in intravital microscopy corresponds to the brush border (Fig. 3). We find its breadth to be 2–3 μm, and it shines particularly brightly in early proximal tubules. With the electron microscope, Maunsbach [16] and Rostgaard and Thuneberg [145] found brush border microvilli 3–4 μm long in early and 1–2 μm long in late proximal convoluted tubule segments. Leyssac

Fig. 4. In vivo microphotograph of the renal cortex surface of a rat during passage of the fluorescent dye lissamine green-rhodamine

[102] believes that the outer not the inner margin of the "white zone" is the limit of the lumen. He interprets the "white zone" as due to reflection of light at the brush border-tubular fluid interface. We cannot agree with this for the following reason: We obtain the same measurement of tubular lumen diameter both when we visualize a segment of proximal tubule in dark field and subsequently when we photograph the same segment during the passage of a fluorescent dye. With fluorescence microscopy there is no incident light reflection (Fig. 4). Thus, the "white zone" corresponds to the brush border, and its inner margin defines the proximal tubule lumen.

Table 1 surveys data from the literature on the diameter of the proximal tubule lumen of nondiuretic rats measured with a variety of techniques. Tables 2 and 3 report the effects of diuretic agents and increased ureteral pressure, respectively, on proximal lumen diameter in the rat. Table 4 summarizes proximal lumen diameter measurements in other species.

Under control conditions of antidiuresis, proximal lumen diameter in the fully grown rat is about 20 microns (Table 1). Lumen diameter increases with the size of the rat as shown by data of Steinhausen *et al.* [175] and Leyssac [100] (Table 1). Proximal lumen diameter is increased by injection of oil for a split-drop determination, so measurements in this condition do not give normal values [166]. The diameter measurements by Brunner *et al.* (Tables 1 and 3) were made in tubules dilated by castor oil injection.

Table 1. Lumen diameters of proximal tubules of rats under nondiuretic control conditions

Diameter (μ)	Rat strain	Weight (g)	Sex	Technique	Reference
14–24	Wistar	160–300		Incident light microphotography	Wahl *et al.* [198]
15.7 ± 1.18		ca. 200		Incident light microphotography	Thurau and Deetjen [191]
16.4 ± 1.8	Wistar	70–80	♂	Incident light microphotography (kidney surface rinsed with Tyrode)	Steinhausen *et al.* [175]
22.8 ± 0.66	Wistar	300–330	♂	Incident light microphotography (kidney surface rinsed with Tyrode)	
19.8 ± 0.62	Albino	250–340	♂	Incident light microphotography (kidney surface rinsed with mineral oil)	Steinhausen [166]
17.0 ± 0.4	FW49	200–300	♂	Incident light, graduated ocular	Krause *et al.* [90]
18.5 ± 0.4	Albino	250–350	♂	Incident light microphotography	Koch *et al.* [89]
18.7 ± 0.3	Wistar	220–270	♂	Incident light microphotography	Baines *et al.* [8]
19.0 ± 1.3	Albino	95–110	♂	Snap-freezing	Leyssac [100]
27.1 ± 0.7		250–300	♂		
19.3	Albino			Incident light microphotography	Walther and Schoeppe [202]
19.3 ± 0.5	Albino	180–220	♂	In vivo fixation with osmium, histology, electronmicroscopy	Langer *et al.* [94]
19.4 ± 0.4		180–240		Incident light microphotography	Wahl *et al.* [197]
19.5 ± 1.4	Albino	230–290		Incident light microphotography	Deetjen [40]
19.6 ± 2.01		180–220	♀	Calculated from GFR, reabsorption, passage time, etc.	Heller and Nováková [80]

Values are means ± SE.

Table 1 (continued)

Diameter (μ)	Rat strain	Weight (g)	Sex	Technique	Reference
19.8 ± 0.2	Wistar	270–390	♀	In vivo fixation, histology	Walther and Lindemann [201]
20	Wistar	150–470	♂	Incident light, estimated	Gottschalk and Mylle [68]
20.4	Wistar	302, 345	♀, ♂	Snap-freezing, microdissection	Baines and de Rouffignac [7]
21.4 ± 0.3	Wistar			Incident light	Mályusz *et al.* [112]
21.6 ± 0.6	Sprague-Dawley	160–350	♂	Snap-freezing	Hayslett *et al.* [77]
24.0 ± 2.71		200–250	♀	Incident light microphotography	Heller and Nováková [81]
24.4 ± 0.24	Albino	250–320	♂	Incident light, microperfusion (24 nl/min)	Wiederholt *et al.* [211]
26–28	Albino	ca. 250	♂	Incident light (includes brush border)	Bojesen and Leyssac [16]
33.6 ± 2.2 SD	Sprague-Dawley			Incident light microphotography; split-drop experiment	Brunner *et al.* [29]

A reduction in glomerular filtration rate leads to a decrease in proximal lumen diameter in the cat [176]. Similar findings were reported by Rector *et al.* [138] in the rat, but Wahl *et al.* [197] have published opposite results. Because of the suggestion [61, 63] that changes in tubular geometry might affect tubular fluid reabsorption and thereby play a role in glomerular-tubular balance, proximal diameter measurement have aroused considerable interest. A detailed discussion of this subject may be found in the article by Gertz [127].

Diuretics, by inhibiting fluid reabsorption, generally induce an increase in proximal tubular hydrostatic pressure and diameter (Table 2). The degree of dilation usually parallels the intensity of the diuresis. Due to the limited capacity of the collecting duct system [69], a large increase in urine flow leads to a rise in tubular hydrostatic pressure and diameter. The extent of dilation also depends on possible effects of the diuretic agent on glomerular filtration rate and interstitial fluid pressure. Cortell *et al.* [37] found that proximal lumens dilated more during a furosemide-induced diuresis than during a mannitol-induced diuresis of similar magnitude, a difference which they ascribe to a greater increase in interstitial fluid pressure during

Table 2. Lumen diameters of proximal tubules of rats during diuresis

Diameter (μ)	Diuretic	Rat strain	Weight (g)	Sex	Technique	Reference
16.2 ± 1.36	Mannitol		ca. 200		Incident light	Thurau and Deetjen [191]
22.7 ± 0.8	Furosemide	Albino	230–290		Incident light	Deetjen [40]
23.6 ± 2.11	Saline		180–220	♀	Calculated	Heller and Nováková [80]
25.0 ± 0.7	Hydro-chloro-thiazide	FW49	200–300	♂	Incident light	Krause *et al.* [90]
26.6	Saline	Wistar	190–450	♂	Calculated	Arrizurieta-Muchnik *et al.* [4]
27.6 ± 0.8					Incident light	
27.1 ± 0.8	Saline	Sprague-Dawley	160–350	♂	Snap-freezing	Hayslett *et al.* [77]
27.6 ± 0.9	Tyrode	Albino	250–340	♂	Incident light	Steinhausen [166]
27.7 ± 0.55	Mannitol	Wistar	300–330	♂	Incident light	Steinhausen *et al.* [175]
33.1 ± 0.5	DOCA and salt hyper-tension	Wistar	180–220	♀	Incident light	Mályusz *et al.* [112]
35	Hypertonic dextrose	Wistar	150–470	♂	Incident light	Gottschalk and Mylle [68]
38.0 ± 1.3	Furosemide	FW49	200–300	♂	Incident light	Krause *et al.* [90]

Values are means ± SE.

Table 3. Lumen diameters of proximal tubules of rats during increased ureteral pressure[a]

Diameter (μ)	Ureteral pressure (mm Hg)	Diuretic	Rat strain	Weight (g)	Sex	Reference
25.6 ± 0.84	40	—	Albino	250–340	♂	Steinhausen [166]
37.4 ± 0.96	40	Tyrode				
35.0 ± 0.28	25	—	Sprague-Dawley			Brunner *et al.* [29]
39.6 ± 0.30	40	—				

Values are means ± SE.
[a] Diameters were measured from incident light microphotographs.

Table 4. Lumen diameters of proximal tubules of other mammals

Species	Diameter (μ)	Condition	Weight	Technique	Reference
Mouse	23.8 ± 1.2	Mannitol and Stop flow	10 – 18 g	Snap-freezing	Bordier *et al.* [17]
Psammomys	12.7 ± 0.6	Antidiuresis	81 –117 g	Snap-freezing, microdissection	Baines and de Rouffignac [7]
Cat	17.2 ± 0.7	Antidiuresis	2.5 – 2.8 kg	Incident light microphotography	Steinhausen *et al.* [175]
	17 –23	Tyrode	1.45– 2.5 kg		Steinhausen *et al.* [176]
	25.7–27.7	Mannitol	2.5 – 2.8 kg		Steinhausen *et al.* [175]
Dog	24.6	Antidiuresis	13.0 –21.2 kg	Incident light microphotography	Knox *et al.* [88]
	28.0	Furosemide			
	30	Antidiuresis	ca. 24 kg	Incident light microphotography	z. Winkel *et al.* [218]
	35	Elevation of ureteral pressure (60 cm H_2O)			

a mannitol diuresis. With a maximal diuresis, most observers would accept a dilatation of the lumen of about 40% of the control value.

An increase in ureteral pressure will increase tubular pressure and thereby dilate proximal lumens (Table 3). The effectiveness of this measure depends on the urine flow rate. A combination of increased ureteral pressure and diuretic most rapidly produces a persistent massive dilation of the tubules. An increase in outflow resistance, caused by too narrow a ureteral cannula, may also induce tubular dilation [36].

C. Distal Tubule Lumen Diameter

Table 5 summarizes distal lumen diameters in the rat. Distal tubule lumens are narrower than proximal lumens, reflecting their lower distending internal pressure. A small change in internal or external pressure will produce a large change in distal tubular diameter. For example, an increase in internal hydrostatic pressure from 7 to 12 mm Hg will double the lumen

Table 5. Lumen diameters of distal convoluted tubules of rats

Diameter (μ)	Condition	Rat strain, Weight (g), Sex	Technique	Reference
9.35 ± 2.65	Antidiuresis	ca. 200	Incident light	Thurau and Deetjen [191]
18.8 ± 2.28	Mannitol			
16.9 ± 0.3	Antidiuresis	Wistar, 270–390, ♀	In vivo fixation, histology	Walther and Lindemann [201]
18.1 ± 1.31	Antidiuresis	Wistar, 300–330, ♂	Incident light microphotography	Steinhausen *et al.* [175]
30.4 ± 1.71	Mannitol			

diameter [37]. With an osmotic diuresis, distal tubule diameters increase relatively more than proximal diameters. An increase in interstitial fluid pressure may cause collapse of distal tubules. This is probably the explanation for the temporary collapse of distal tubules after terminating acute renal artery occlusion [163] (Fig. 3). During acute temporary interruption of glomerular filtration, distal tubules, in contrast to proximal tubules, do not collapse (Fig. 3), probably due to the lower rate of fluid reabsorption in the distal tubule [175].

III. Tubular Passage Time

A. Techniques

1. Measurements by Intratubular Dye Injection

Tubular passage time, or tubular transit time, is the time it takes for fluid to move along a given segment of the nephron. The first measurements of tubular passage time were obtained by micropuncture and injection of dye into a loop of a proximal tubule. Thurau and Deetjen [191] used the dye indigo carmine for this purpose. Solomon [156] attempted this measurement with dyed oil droplets. The results from both of these studies were variable, and it is likely that the tubular urine flow rate was uncontrollably altered with this technique.

2. Measurements by Intravascular Dye Injection

The introduction into renal physiology of the dye lissamine green (LG) made possible the routine measurement of passage times on the kidney surface [160]. This dye is given as a bolus injection intravascularly, is filtered by the glomeruli, and passes as a colored wave down the nephron.

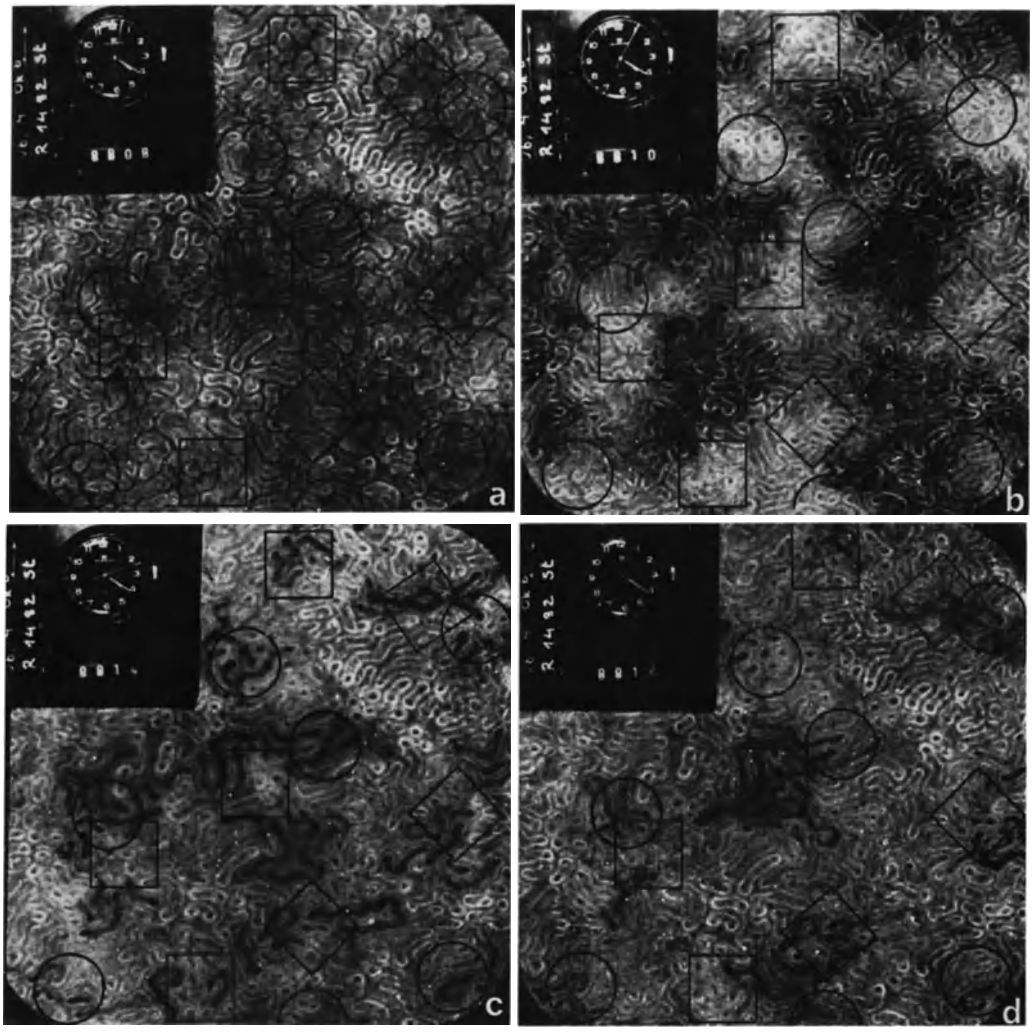

Fig. 5. Low power microphotographs of the renal cortex surface of a rat during a LG passage time determination. The welling points are marked by different symbols. (a) 2.5 sec after LG injection: The dye appears in the welling point and peritubular capillaries. (b) 5 sec after LG injection: The dye passes through the early proximal tubules, which are located at a distance from the welling point. (c) 12 sec after LG injection. (d) 15 sec after LG injection: The dye passes through the late loops of the proximal convoluted tubules, which are located around the welling point

Fig. 6. Low power microphotographs of the renal cortex surface of rat during a LG passage time determination. (From Steinhausen [160].) (a) Dye passage from the welling points to the peritubular capillaries. (b) Dye passage through the early proximal tubule loops, i.e. those near the glomeruli. (c) Dye passage through the middle of the proximal convoluted tubules. (d) Dye passage through the late proximal tubule loops. (e) Disappearance of dye from the renal surface, as the dye traverses the loop of Henle. (f, g, h) Dye passage through distal convoluted tubule loops, marked by arrows

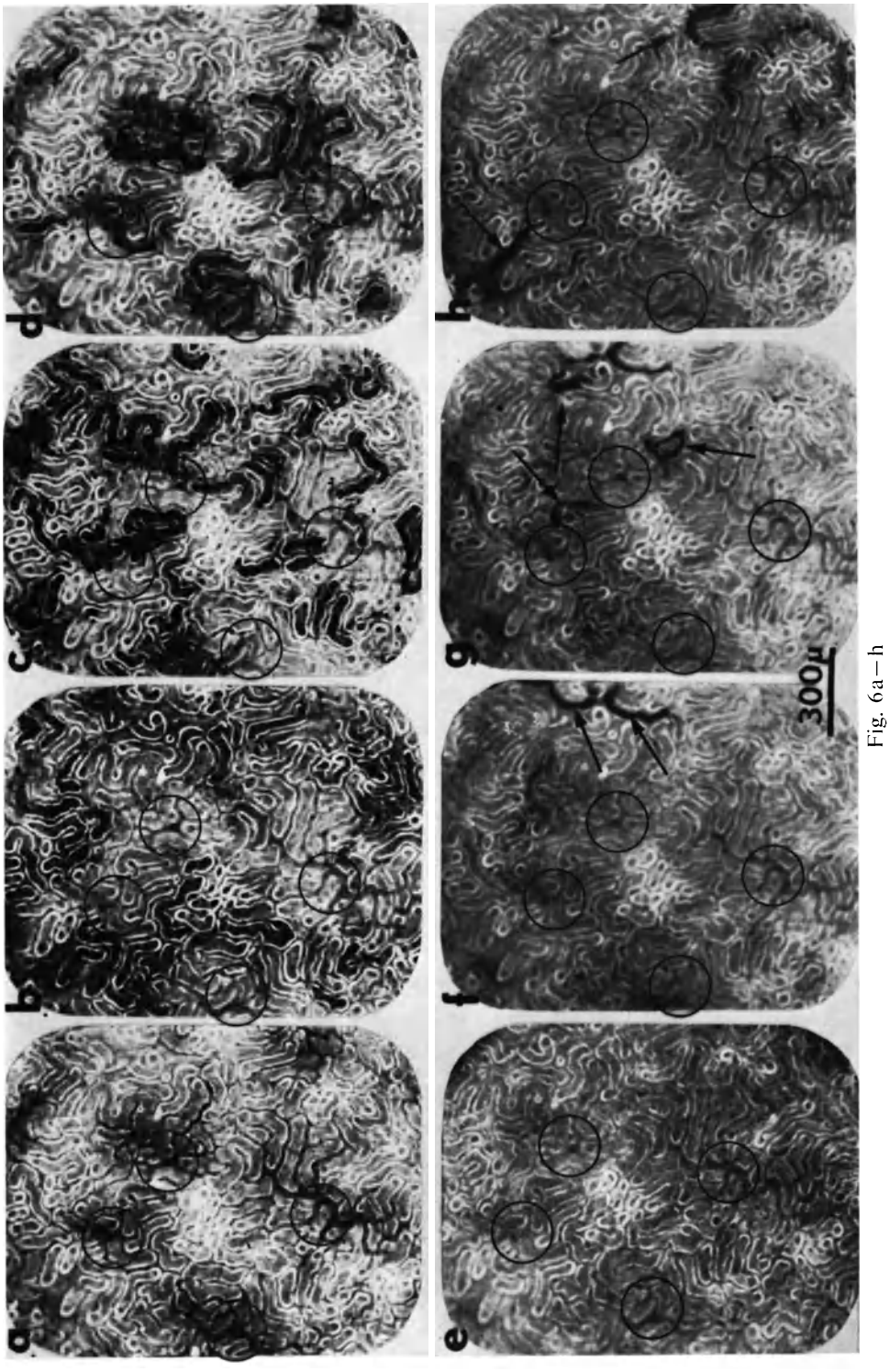

Fig. 6a–h

Table 6. Synonyms, structural formulas, and molecular weights of dyes related to lissamine green SF (From Parekh *et al.* [131])

Synonyms	Structure formulae	Molecular weights
Lissamine Green SF		793
Acid green G Acilan green SFG Light green SF (yellowish) Sulfo green J	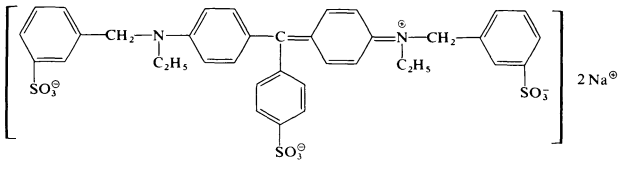	
FD + C Green No. 3		809
Fast green FCF CI Fast green No. 3	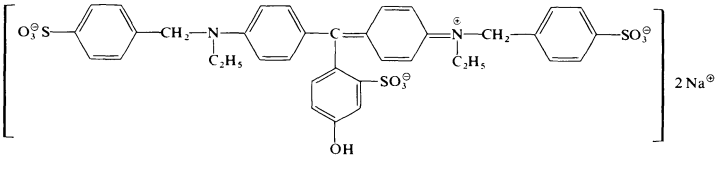	
Lissamine Green V		561
Acid green Alkali fast green A Kiton green V Naphthalene green V	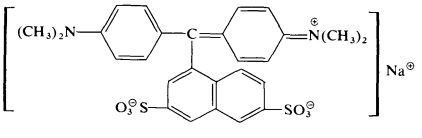	
Lissamine Green BN		577
Acid green SS Java green S Water green SX Wool green S	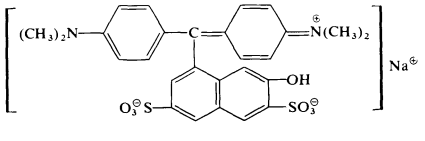	
Kiton Pure Blue V		567
Alphazurine 2G Brilliant acid blue VS Disulphin blue VN Patent blue V	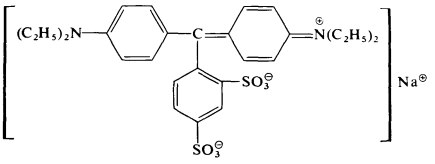	

The progression of the dye can be observed and photographed by incident light microscopy (Figs. 5, 6). Passage times can be estimated from the appearance and disappearance times of the dye in the individual structures on the kidney surface. A critical analysis of this widely used method will be undertaken in this section.

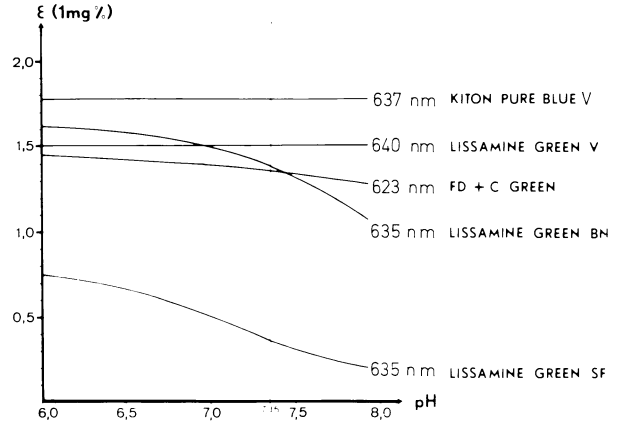

Fig. 7. pH dependence of dye extinction at the absorption maxima of some dyes related to lissamine green SF. (From Parekh *et al.* [131])

B. Properties of Lissamine Green

There is not one lissamine green dye, but several. The lissamine greens are triarylmethane derivatives. Three lissamine greens and two related dyes are listed in Table 6; this table gives common synonyms, structural formulas, and molecular weights [131]. All of these dyes are non-toxic and have quite similar properties in animal experiments [35, 137].

Lissamine green SF (LG SF) was first synthesized in the Badische Anilin and Soda-Fabriken (BASF) by Köhler in 1879 [155] and was used as a textile dye and food color under the name "light green SF". The dye has been used for staining proteins in electrophoresis methods [18, 38, 44], in tumor studies [67], and as an intravital stain in cell research [86]. We became aware of this dye through the work of Müller [122], who used it in his study of capillary permeability in the frog web.

The physical and chemical properties of LG SF and related dyes were investigated by Parekh *et al.* [131]. In addition to LG SF they studied the following dyes (Table 6): FD + C Green No. 3 (FD + C 3), lissamine green V (LG V), lissamine green BN (LG BN), and kiton pure blue V (KPB V). When the color intensities of the dyes are compared in solutions of the same concentration by weight at pH 7.35, they increase in the order LG SF, FD + C 3, LG BN, LG V, and KPB V (Fig. 7). Like most triarylmethane dyes, LG SF changes its color intensity with pH [73, 131, 174], as is also shown in Fig. 7. LG V and KPB V, however, do not change their extinctions in the physiological pH range (Fig.7). For passage time determinations, a dye should be readily filtered by the glomeruli, and hence bound to a minimal extent by plasma proteins. All of the dyes examined are reversibly bound to plasma proteins. The ultrafiltrability of the dyes from fresh rat plasma was

examined in vitro, and was found to increase roughly in the order LG SF, FD+C 3, LG BN, LG V, and KPB V. For example, at a plasma concentration of 200 mg/100 ml dye, 28% of LG SF is free (i.e. ultrafiltrable) and 56% of KPB V is free. LG SF shows the peculiar property of reacting irreversibly with plasma proteins to form a colorless compound. This reaction is advantageous when repeated i.v. injections of LG SF are given, since the animal will not become intensely dyed. However, the formation of a colorless compound makes the accurate determination of intratubular concentrations difficult. For a number of reasons KPB V is particularly recommended: a) it has a high color intensity, b) its extinction is pH insensitive, c) it has a high ultrafiltrability, d) it does not form a colorless compound, and e) it has a bluish tinge which provides a good optical contrast against the red blood vessels of the kidney.

C. Necessary Conditions for Determining Passage Times by Intravascular Dye Injection

There are three basic conditions which must be fulfilled for the accurate determination of passage times by intravascular dye injection.

(1) All nephrons on the kidney surface must have a similar blood flow rate, i.e. the dye passage should begin simultaneously in all surface nephrons. Under normal control conditions this requirement is fulfilled, since the dye arrives uniformly in all vessels on the kidney surface. This is because there are no "resting" or "inactive" nephrons in normal, anesthetized mammals. The situation is different, however, during experimental stimulation of the renal nerves [178, 179]. In this case, some regions of the kidney cortex surface are completely cut off from their blood supply, while other regions are perfused almost normally. Under pathophysiological conditions blood flow to the kidney surface may be quite non-uniform.

(2) The dye must enter the tubule lumens solely by glomerular filtration, i.e. it must not be secreted. We have directly observed LG filtration in superficial glomeruli [170]. During passage of LG downstream, each loop of a tubule is stained in turn [160], implying that there is no entry of LG into the tubule lumen via tubular secretion. Popa *et al.* [137] found in clearance studies in rats that the clearances of LG and related dyes, corrected for protein binding, are identical to the inulin clearance (e.g. Fig. 8). Since LG is not secreted, it is clear that the tubular passage of this dye results from glomerular filtration.

(3) The injection of the dye must not alter the tubular urine flow. In this regard, two possible sources of error require comment.

First, measurements of passage time will be inaccurate if the arterial blood pressure changes upon injection of the dye. A fall in blood pressure will decrease the tubular urine flow rate, and vice versa. Acute changes in

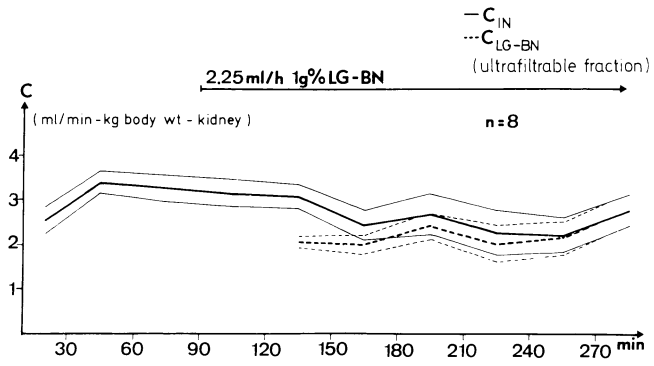

Fig. 8. Means and standard errors of inulin and lissamine green BN clearances in experiments on rats. The dye is not secreted by the kidney tubules

blood pressure can be avoided by using freshly prepared, isoosmolar, and isohydric solutions of purified dye, and by using a minimum volume for the bolus injection. In large animals (cats and dogs), the insertion of an aortic cannula is recommended, so that high concentrations of dye can enter the renal artery directly [176]. We monitor blood pressure routinely during dye injections.

Second, the dye must not influence tubular fluid reabsorption since this would also alter the tubular urine flow and change the passage time. The finding that LG decreased the short-circuit current in the frog skin [35, 45] and had diuretic and natriuretic effects in the rat [79, 143] suggested an influence on tubular reabsorption. The natriuretic effects of LG were investigated further. It was found that these effects appeared only with amounts of LG which exceed those necessary for passage time determinations [60, 108, 119]. Elmer and Leyssac [48] found that a single LG injection produced no immediate change in tubular reabsorption. We found that commercial LG is often contaminated by large amounts of sodium sulfate, and other unknown impurities, a fact not adequately considered by previous workers. The natriuretic effect of LG dyes can be minimized by removal of these impurities [131; 131a].

In conclusion, the requirements for accurate passage time measurements appear to be fulfilled by the method of intravascular bolus injection of purified LG dye in animals with normal kidneys.

D. Passage Time Determinations with LG

While the kidney cortex surface is observed through a light microscope, a bolus of LG is injected i.v. One can see and time the following events (cf. Table 7, upper half):

Table 7. Appearance and disappearance times on the renal cortex surface of intravascularly injected lissamine green dye, and derived tubular passage times. Data from nondiuretic control rats, cats, and dogs [162, 166]. The dye was injected as a bolus into the jugular vein in rats, and into the aorta above the kidneys in cats and dogs

		Rats (ca. 300 g) $N=14$	Cats (ca. 1.5–2.5 kg) $N=15$	Dogs (ca. 24 kg) $N=14$
I.	Beginning of vascular coloration	2.5 ± 0.16	1.0 ± 0.06	2.3 ± 0.2
II.	LG arrival in earliest surface proximal tubule loops	4.9 ± 0.26	5.4 ± 0.47	6.8 ± 0.4
III.	LG arrival in the last superficial loops of the proximal tubule	13.2 ± 0.57	12.0 ± 0.47	18.3 ± 1.1
IV.	Disappearance of dye from all surface proximal tubules	21.2 ± 1.56	17.0 ± 1.2	25.8 ± 2.0
V.	LG arrival in first superficial distal convoluted tubules	44.2 ± 4.14	49.0 ± 3.7	56.1 ± 3.9
VI.	Disappearance of dye from over 90% of the superficial distal tubules	83.5 ± 8.12	90.0 ± 5.9	88.9 ± 7.4
	Glomerular-surface passage time (II minus I)	2.4 ± 0.19	4.4 ± 0.3	4.5 ± 0.3
	Passage time for the proximal tubule visible on the surface (III minus II)	8.3 ± 0.42	6.6 ± 0.4	11.5 ± 0.8
	Proximal passage time (III minus I)	10.7 ± 0.51	11.0 ± 0.3	16.0 ± 0.7
	Loop of Henle passage time (V minus III)	31.0 ± 3.66	37.0 ± 2.6	37.8 ± 2.5
	Distal passage time (VI minus V)	39.3 ± 5.48	41.0 ± 3.1	32.8 ± 5.7

Values are means (in seconds) ± SE.

I. Beginning of vascular coloration, starting from the welling point. At this time, the dye has already passed the glomeruli. If a glomerulus happens to be visible on the surface, one can observe that the dye appears in the glomerulus an instant before it reaches the welling point [160].

II. LG arrival in the lumens of the earliest superficial proximal tubule loops.

III. LG arrival in the last superficial loops of the proximal tubule. These are usually situated in a circle around the welling point.

IV. Disappearance of dye from all surface proximal tubules.

V. LG arrival in surface distal convoluted tubules. Individual distal tubules are colored early or late, depending chiefly on the length of the distal convolutions [149, 160, 220]. In Table 7, only the earliest distal appearance times are listed.

VI. Disappearance of the dye from over 90% of the superficial distal convoluted tubules. During intense antidiuresis or other experimental conditions, dye may linger in individual distal tubules. This approximate time has proved useful.

The following tubular passage times can be calculated from the above measurements (cf. Table 7, lower half):

From II minus I: glomerular-surface passage time (i.e. the transit time through the initial part of the proximal tubule hidden below the kidney surface).

From III minus II: passage time for the proximal tubule visible on the kidney cortex surface.

From III minus I: proximal passage time. Gertz *et al.* [63] suggested this simple determination. Originally, we calculated proximal passage time from IV minus II, taking into consideration the mean duration of dye coloration of individual proximal loops [160].

From V minus III: loop of Henle passage time.

From VI minus V: distal passage time.

E. Accuracy of Passage Time Measurements

Measurement of passage times would be more exact if the dye stained fluid moved as a sharply demarcated color front down the tubule. However, this does not occur. One reason is that flow down the tubule is probably laminar. We previously calculated a Reynolds number of 0.014 for the proximal convolution; turbulence usually develops with numbers greater than 1200. As a consequence of laminar flow, the velocity of dye stained fluid is higher in the center of the tubule lumen. If there were ideal laminar flow, then the color front would be spread over several proximal loops during a passage time of 10 sec [162]. This condition is probably not attained because the tortuous structure of the tubule prevents ideal laminar flow. Also, flow down the tubule differs from simple Poiseuille flow because of absorption of fluid through the tubule walls. A second factor responsible for lack of a sharp color front is radial diffusion. For distances equal to tubular radii, diffusion of dye molecules from the center to the wall of the

tubule probably takes place in less than half a second [124]. Radial diffusion reduces the dye intensity of the color front as fluid moves down the tubule. As a consequence of laminar flow and radial diffusion, neat color fronts are not observed, but only more intensely stained moving zones of color are seen[1].

Some subjective factors may influence the accuracy of passage time measurements. The experience and reaction time of the observer must be considered. It is always best if a single observer measures passage times under different experimental conditions. A minimal reaction time of 0.2 sec must be allowed [193]; however, this error is small, since passage times are determined from time differences. Animal preparation and microscopic techniques will also influence passage time values.

There are several ways of increasing the accuracy of passage time measurements. For visual observations, we have found that using an automatic timer results in more accurate measurements than reading a stopwatch. Also, changes in passage time are always most accurately recorded if the same microscopic field is observed under different experimental conditions. Finally, the accuracy of passage time measurements can be increased practically at will by the frame-by-frame evaluation of a movie filmed during dye passage. Accuracy then depends on the picture frequency, microscopic enlargement, and photographic techniques.

F. Do We Measure a Mean Passage Time?

The passage time through an "average" nephron is not usually recorded. Rather, extreme values are noted, e.g. the arrival of dye in the first proximal loop of a nephron situated very close to the surface, or the disappearance of dye from a very long proximal convoluted tubule. In general, the larger the microscopic field (or the lower the magnification), the greater the chance of seeing more extreme values. The size of the microscopic field is particularly important in cases where there is a marked heterogeneity of nephron function. Under control conditions, proximal passage times in different nephrons are similar, so a mean passage time is nearly approximated. However, in pathophysiological conditions, individual nephron passage times may be markedly heterogeneous, and estimates such as "the dye has passed most of the proximal tubules" are more appropriate. Loop and distal passage times are quite heterogeneous even in the normal kidney, due to differences in tubule lengths and the low volume flow rate. Therefore passage times estimated here are even less representative of an "average" nephron.

[1] Higher flow velocities in the center of the tubular lumen could also not be found by analyzing a fluorescent color front using a high intensity television system (M. Steinhausen, H. Wayland and J. Fox. Pflügers Arch. ges. Physiol., in press).

G. Results of Measurements of Passage Times under Control Conditions

Table 7 summarizes passage time measurements in rats, cats, and dogs under nondiuretic control conditions. The data are partly taken from some of our earlier studies [162, 166] and partly assembled from their protocols. Passage times are similar in these different mammals. The longer tubule length and greater tubule lumen diameter in the dog compared to the rat (these factors prolong the passage time) are counterbalanced by a higher single nephron glomerular filtration rate in the dog (this shortens the passage time).

Table 8 surveys proximal passage time measurements (III minus I) in rats under control conditions obtained by other authors. Most investigators have limited themselves to proximal passage time determinations, since the proximal tubule is of special importance in glomerular-tubular balance

Table 8. Proximal passage times in rats during nondiuretic control conditions

Time (sec)	Strain[a]	Weight (g)	Sex	Technique	Reference
7.1 ±0.85 SD	S	200–250	♂	10% LG, pH 7	Fülgraff *et al.* [58]
8.9 ±0.3 SD	S			10% LG, pH 2	
8.4 ±0.2	S	180–230	♂	10% LG, pH 7, 0.01 ml	Fülgraff and Meiforth [59]
9.0 ±0.3	S	180–220	♂	LG	Greven and Fülgraff [71]
9.0 ±1.1		180–220	♀	LG	Heller and Nováková [80]
9.0 ±0.20	S	190–260		LG, with fluid-replacement	Brunner *et al.* [29]
10.2 ±0.26				LG, no fluid-replacement	
9.2 ±0.4	CR	200–260	♂	LG	Cortell *et al.* [36]
9.2 ±1.1	W	150–200	♂, ♀	10% LG, pH 7.4, 0.02–0.03 ml	Armsen *et al.* [3]
9.3 ±0.3	S, LE	170–300	♂	LG	Anagnostopoulos *et al.* [1]
9.43 ±0.27		185–210	♀	10% LG, 0.04 ml	Heller [79]
9.6 ±0.4	FW49, CR	150–200	♂	LG, 0.05 ml	Hierholzer *et al.* [85]
9.6 ±0.04		ca. 275	♂	LG	Buentig and Earley [30]
9.6 ±1.1	W	160–300		LG	Wahl *et al.* [198]

Table 8. (continued)

Time (sec)	Strain[a]	Weight (g)	Sex	Technique	Reference
9.69 ± 1.1	SD DI	150–300	♂, ♀	5% LG, buffered	Schnermann *et al.* [152]
9.7 ± 0.3		180–240		5% LG, buffered	Wahl *et al.* [197]
9.73 ± 0.42		190–220	♀	5% LG, 0.02 ml	Heller [78]
9.8 ± 0.5	S	240–310	♂	10% LG, 0.05 ml	Brenner *et al.* [22]
9.9 ± 0.34	W	180–200	♀	5% LG, 0.05 ml	Stumpe *et al.* [182]
9.9				LG	Frömter and Hegel [56]
10.0 ± 0.12	S	180–220	♂	LG	Fülgraff and Heidenreich [57]
10.3 ± 0.3	W	180–220	♀	LG	Mályusz *et al.* [112]
10.3 ± 0.4	S	200–400	♂	10% LG	Weinman *et al.* [206]
10.4 ± 0.5	A	220–390	♂	10% LG	Yarger *et al.* [222]
10.4 ± 0.2	W	160–230	♂	LG	Frohnert *et al.* [55]
10.9 ± 0.2	W	160–230	♀	LG	
10.4 ± 0.48	S	200–275	♀	LG	Rodicio *et al.* [144]
10.5 ± 0.27	W	180–450	♂	LG	Schnermann *et al.* [151]
10.6 ± 0.04		200–300	♂	10% LG, 0.05 ml	Landwehr *et al.* [93]
10.7 ± 0.85	W	190–450	♂	5% LG, 0.05 ml	Arrizurieta-Muchnik *et al.* [4]
10.7 ± 0.04	S	200–300	♂	10% LG, 0.05 ml	Falchuk *et al.* [51]
10.8 ± 0.24	W	180–210	♀	5% LG, 0.05 ml	Lowitz *et al.* [107]
11.0 ± 0.3	S	180–220	♂	10% LG	Thoenes *et al.*[190]
11.6 ± 0.51	A	200–350	♂	5% LG, 0.1 ml	Malnic *et al.* [110]
12.0 ± 0.7	FW49	200–300	♂	LG	Krause *et al.*[90]
12		20 days old		LG	Čapek *et al.* [33]
12 ± 1		200–400		10% LG, low salt diet	Henry *et al.* [82]
13 ± 1				10% LG, high salt diet	
12.2 –12.5				LG	Rector *et al.* [139]
12.8 ± 0.7		160–350	♂	10% LG, 0.05 ml	Hayslett *et al.* [77]
15	white	ca. 250	♂	10% LG, 0.05 ml	Bojesen and Leyssac [16]

Values are means ± SE.

[a] A = Albino, CR = Charles River, DI = Hereditary Diabetes Insipidus, LE = Long-Evans, S = Sprague-Dawley, W = Wistar.

Table 9.
Distal arrival times of lissamine green in rats during nondiuretic control conditions

Time (sec)	Strain[a]	Weight (g)	Sex	Technique	Reference
31.4 ±0.9	S	180–230	♂	10% LG, pH 7, 0.01 ml	Fülgraff and Meiforth [59]
33.9	S, FW49	160–320		LG	Frömter and Hegel [56]
39 ±0.6	S	210–330	♂	FD + C green	Bello-Reuss *et al.* [15]
41.4 ±1.5	S, LE	170–300	♂	LG	Anagnostopoulos *et al.* [1]
42.5 ±5.2	W	150–200	♂, ♀	10% LG, pH 7.4, 0.02–0.03 ml	Armsen *et al.* [3]
44.2 ±1.2		220–390	♂	10% LG	Yarger *et al.* [222]
66.9 ±2.4	S	160–350	♂	10% LG, 0.05 ml	Hayslett *et al.* [77]
71.3 ±5.5	W	250–300	♂	2% LG, 1.25 ml kg	Roch-Ramel *et al.* [141]

Values are means ±SE.
[a] LE = Long-Evans, S = Sprague-Dawley, W = Wistar.

Table 10. Loop passage times (V minus III, cf. Table 7) under control conditions

Time (sec)	Species	Weight	Sex	Technique	Reference
23.0 ±0.77	Sprague-Dawley rat	180–230 g	♂	10% LG, pH 7, 0.01 ml	Fülgraff and Meiforth [59]
28.3 ±1.24	Wistar rat	180–200 g	♂	5% LG, 0.05 ml	Stumpe *et al.* [182]
60.0	Wistar rat	250–300 g	♂	2% LG, 1.25 ml kg	Roch-Ramel *et al.* [141]
32.3 ±1.06	Dog	3.5–35 kg		10% LG, buffered, i.a.	Liebau *et al.* [103]

Values are means ±SE.

(see Gertz in Ref. [127]). The values fluctuate around a mean of 10 sec, which agrees with our own observations. The differences in results among the authors may reflect differences in rat strain, anesthesia, technique of animal preparation, microscope magnification, reading method, etc. "Control conditions" represent the individual controls of the particular investigator, and may differ from laboratory to laboratory.

The arrival of the test dye in the earliest loops of the distal convoluted tubule (Tables 7 and 9) and the derived loop of Henle passage time (V minus III) (Tables 7 and 10) are easy to determine. However, normal values will be observed only if there is unhindered drainage of the ureter. In a highly concentrating kidney (e.g. $U/P_{inulin} = 600$), if too much dye is injected, LG may precipitate in the collecting ducts and impede the outflow of urine.

H. Alterations of Tubular Passage Time and the Factors Involved

Tubular passage time is an expression of the linear velocity of fluid flow in a given length (or segment) of the nephron. Passage times are determined basically by the following factors:

a) glomerular filtration rate,
b) rate of tubular fluid reabsorption,
c) tubular lumen diameter, and
d) outflow resistance or ureteral pressure.

If each factor is examined individually, the following effects can be predicted from hydrodynamic principles:

a) an increase of glomerular filtration rate alone will shorten the passage time, and a decrease will prolong it;

b) an increase in tubular fluid reabsorption alone will prolong the passage time, and a decrease will shorten it;

c) an increase in tubular diameter alone will prolong the passage time, and a decrease will shorten it; and

d) an increase in outflow resistance or ureteral pressure alone will prolong the passage time, and a decrease will shorten it.

The four factors are interdependent, so that alteration of one factor alone almost never occurs, and this may create a complicated situation. For example, a primary increase in glomerular filtration rate would be expected to shorten the proximal passage time. However, increased fluid filtration results in an increased intratubular pressure, and consequently an increase in proximal tubule diameter. This would prolong the passage time. An increase in glomerular filtration rate also leads to an increase in proximal fluid reabsorption ("glomerular-tubular balance"), and this prolongs the passage time. It is clear that the primary result of the increased glomerular filtration rate, a shorter passage time, is considerably blunted by other effects.

Tables 11 and 12 summarize proximal passage time measurements in rats and dogs, respectively, in a variety of diuretic states. In a saline diuresis, proximal passage time is usually shortened, due to an increase in glomerular filtration rate and decreased proximal fluid reabsorption. The same occurs during a urea diuresis [141, 142]. Inhibition of tubular reabsorption may not necessarily lead to a shortened passage time. With a very strong diuresis, the resistance of the narrow collecting duct system of the kidney leads to

Table 11. Proximal passage times in rats during different diuretic conditions (saline diuresis, adrenalectomy plus steroid administration, etc.)

Time (sec)	Condition	Reference
6.01 ± 0.5	Isotonic saline, 0.57 ml/min for 60 min	Heller and Nováková [80]
ca. 7	Isotonic saline, 5.7–7.5 ml	Brenner and Berliner [21]
7.0 ± 0.4	Ringer, 0.375 ml/min	Brenner *et al.* [22]
7.1 ± 0.2	Isotonic saline, 0.5 ml/min to 10% BW	Arrizurieta-Muchnik *et al.* [4]
7.3 ± 0.27	Isolated perfused kidney	Bahlmann *et al.* [5]
8.0 ± 0.26	2.5% NaCl, 0.1 ml/min	Stumpe *et al.* [183]
8.1 ± 2.0 SD	Saline	Baines *et al.* [6]
8.4 ± 0.3	Saline, 0.5 ml/min	Bank *et al.* [10]
8.5 ± 0.58	Mannitol	Stolte *et al.* [180]
8.6	Isotonic saline, 0.2 ml/min	Brenner *et al.* [20]
9.2 ± 0.42	Isotonic saline, 0.4 ml/min	Rodicio *et al.* [144]
9.7 ± 0.7	Saline drinking for 4 weeks + Aldosterone	Stumpe and Ochwadt [184]
10.3 ± 0.24	Saline drinking for 4 weeks	
10.1 ± 0.01	Ringer, 0.5 ml/min to 10% BW	Landwehr *et al.* [93]
10.4 ± 0.3	Isotonic saline, 0.5 ml/min	Hayslett *et al.* [77]
11.5 ± 0.7	Adrenalectomy and Cortisone	Wiederholt *et al.* [213]
13.4 ± 0.7	Adrenalectomy and Dexamethasone	
19.5 ± 1.0	Adrenalectomy and Aldosterone	
12.9 ± 0.3	Hypertension induced by DOCA and salt	Mályusz *et al.* [112]
16.3 ± 0.87	Furosemide	Malnic *et al.* [110]

Values are means ± SE.

an increase in proximal tubular pressure [69]. This would a) increase the tubular diameter, and b) decrease the glomerular filtration rate. These changes would favor an increase in passage time. Results with diuretic drugs such as furosemide (Tables 11 and 12) may be explained by such changes.

If the outflow of urine is restricted due to ureteral pressure elevation or a narrow ureteral cannula, proximal tubular pressure and diameter are increased [36, 68, 138]. Glomerular filtration rate falls, and tubular fluid

Table 12. Proximal passage times in dogs

Time (sec)	Condition	Technique	Weight (kg)	Reference
16.0 ± 1.1	Controls	1 ml 10% LG intraaorta	ca. 24	z. Winkel *et al.* [218]
53.1 ± 9.7	60 cm H_2O ureteral pressure			
16.6 ± 0.7	Hydropenia	0.5 ml 10% LG intraaorta	13.0–21.2	Knox *et al.* [88]
35.1 ± 2.8	Hydropenia and Furosemide			
21.6 ± 1.3	Controls	5% LG or FDC-green into renal artery	10–20	Lockhart *et al.* [105]
45.5 ± 3.8	Triflocin			

Values are means ± SE.

reabsorption also decreases [166]. Under these conditions, proximal passage time is prolonged [36, 138, 166]. An increased resistance due to an increase in urine viscosity will also result in prolonged passage times. Figure 9 shows the marked slowing of passage times induced by the intravenous infusion of a filtered low molecular weight dextran[2] [165].

Loop and distal tubule passage times are much more sensitive to changes in glomerular filtration rate, tubular fluid reabsorption, and outflow resistance than are proximal passage times. This is due primarily to the lower volume flow rates in more distal parts of the nephron. Steinhausen *et al.* [176] found that lowering the arterial blood pressure markedly slows loop and distal passage times. Loop passage time is shortened in the unclamped kidney of rats with Goldblatt hypertension [106, 181, 182, 183]. This is apparently due not only to decreased fluid reabsorption by the loop, but also may reflect a decreased loop diameter due to compression by the blood vessels. Finberg and Peart [53] found that intravenous angiotensin II increased the passage time. This result suggested a decrease in glomerular filtration rate in superficial nephrons. In microperfusion experiments Schnermann [149] saw a decrease of loop passage time (from 52.7 ± 18 to 13.5 ± 3.2 SD sec) when loop perfusion rate was increased from 10 to 48 nl/min. Variations in contact time within the loop and distal tubule could influence water reabsorption by these segments. An increased passage time (i.e. longer contact time) would favor osmotic equilibration between tubular and peritubular fluids, and may lead to formation of a more concentrated urine.

[2] In the meantime the photometry of a FITC-dextran bolus with a molecular weight between 3000 and 150000 allowed the direct measurement of the glomerular permeability on the renal cortex of Wistar-Furth rats (M. Steinhausen, H. Wayland and J. Fox, Pflügers Arch. ges. Physiol. in press).

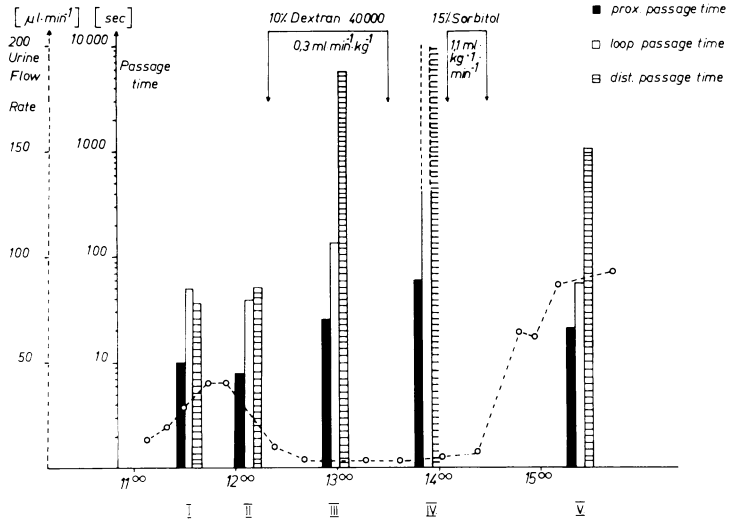

Fig. 9. Prolongation of tubular passage times after i.v. injection of low molecular weight dextran on the cat. (From Steinhausen [165])

I. Tubular Fluid Flow Rate

The volume flow rate of tubular fluid ($\dot{V}$) can be calculated from the following equation: $\dot{V} = \pi r^2 l/t$, where r is the tubular lumen radius, l is the tubular length, and t is the passage time. The measurement of tubular diameter or radius was discussed in Section II. Tubular length is usually determined by nephron microdissection [52, 126, 135]. The measurement of passage time was disscused in this section. Tubular segment length (l) divided by passage time (t) is equal to the linear velocity of tubular fluid flow. Table 13 presents calculated mean flow velocities and volume flow rates for the proximal convoluted tubule under a variety of experimental conditions in rats, cats, and dogs.

Somewhat higher volume flow rates are obtained if these are determined from micropuncture collections of tubule fluid. Wright and Giebisch [221] have reviewed the measurement of single nephron glomerular filtration rate (SNGFR), and report an average value of 40 nl/min in the superficial proximal tubules of adult rats under nondiuretic conditions. With reabsorption of nearly 2/3rds of the filtrate by the end of the proximal convoluted tubule, volume flow rate would be about 13 nl/min at this point. The mean volume flow rate in the proximal convoluted tubule would then lie between the two extreme values, i.e. between 40 and 13 nl/min. By comparison, the mean volume flow rate calculated from the passage time and tubular volume is only 7.8 nl/min (Table 13).

Table 13. Mean proximal tubular volume flow calculated from tubular dimensions and passage time

Species, Condition	Tubular radius (μ)	Tubular length (mm)	Passage time (sec)	Flow velocity (mm/sec)	Volume flow (nl/min)
Rats, antidiuresis	9.9	4.6[b]	10.7	0.43	7.8
Rats, saline-diuresis	13.8	4.6[b]	8.0	0.58	20.7
Rats, ureteral pressure	12.8	4.6[b]	58.8	0.08	2.4
Cats, antidiuresis	8.6	5.8[c]	11	0.53	7.5
Dogs, antidiuresis	15[a]	10.5[d]	16	0.66	27.8
Dogs, ureteral pressure	17.5	10.5[d]	53.1	0.20	11.4

[a] From z. Winkel *et al.* [218].
[b] Length of superficial proximal convoluted tubule [173].
[c] Length of proximal tubule including pars recta from young cat [157].
[d] Length of superficial proximal tubule [96].

This discrepancy is probably due to two factors. First, it is possible that SNGFR and tubular fluid collection rates are exaggerated by excessive suction [221]. Second, and more important, proximal flow velocity (and volume flow) may be underestimated from the passage time determination because this uses the arrival of the dye in the last proximal loops. Therefore this method regularly uses extreme tubule lengths. Consequently flow velocities will be underestimated when they are calculated from an average tubule length based on microdissection (Table 13).

J. Observations on Tubular Urine Flow in the Awake Rat

Glomerular filtration rate in unanesthetized rats appears to be somewhat higher than in anesthetized animals. This has been found in clearance studies (111a) and in recent studies by Bonvalet *et al.* [16a] using a modified Hanssen ferrocyanide technique [74a]. Steinhausen *et al.* [174a] developed a method for directly observing the renal cortical surface in awake rats, and has used this preparation to examine the effects of Inactin anesthesia. Briefly, the method involves placing one kidney in a specially constructed plexiglass chamber with an air-tight window. The chamber was sewn to the skin of the animal. Cannulas were chronically placed in the abdominal vena cava (for injecting fluids) and the abdominal aorta (for monitoring arterial blood pressure). A day was allowed for recovery from surgery. The rat was restrained in a holder, the chamber window removed, and the kidney was then observed with a Leitz Ultropak microscope.

Table 13a summarizes measurements of lissamine green passage times in awake and Inactin anesthetized rats prepared as described above. Proximal and loop of Henle passage times were definitely prolonged by anesthesia.

Table 13a. Lissamine green passage times in conscious and Inactin-anesthetized rats

	1 Conscious	2 Inactin-anesthesia	2−1 % Difference
Proximal passage time (III minus I)	8.1 ± 0.2 sec (19)	9.6 ± 0.5 sec (16)	+19*
Loop of Henle passage time (V minus III)	21.9 ± 1.0 sec (19)	29.6 ± 1.4 sec (16)	+35**
Distal passage time (VI minus V)	24.6 ± 4.8 sec (7)	25.3 ± 1.6 sec (7)	+3

Values are means ± SE (number of observations). Measurements were made on five rats. * $P<0.01$; ** $P<0.001$.

Proximal tubule lumen diameters (21.5 ± 0.5 microns, $n=49$) and outer diameters (43.4 ± 0.7 microns, $n=38$) in awake rats were identical to values found with anesthesia. Hence, the 19% increase in proximal passage time means a similar decrease in average proximal tubular urine flow rate. This decrease is probably due to a decrease in superficial nephron glomerular filtration in the anesthetized rat.

K. General Use of LG in Kidney Micropuncture

The measurement of LG passage times by intravenous dye injection is probably the simplest and most rapid method used in micropuncture experiments to survey over-all kidney function. Several authors [3, 15, 36, 39, 134, 208] terminate experiments if the proximal passage time exceeds 11–13 sec in control rats. Cortell *et al.* [36] state: "all animals were required to meet the following criteria or the experiment was discontinued and discarded: 1) blood pressure greater than 95 mm Hg, 2) body temperature between 36–39 °C, 3) urine free of gross blood, and 4) transit time less than 13 sec with dye flowing evenly to all areas of the kidneys with no retention of dye in the tubules." Some authors [108, 142, 195] use only micropuncture samples if LG passage times are equal before and after the collection.

Intravascular bolus injection of LG is the simplest way to distinguish early from late portions of the proximal tubule [3, 12, 21, 25, 54a, 55, 106, 125, 146–148, 185, 214], to identify distal tubules on the kidney surface [34, 87, 111, 118, 187, 196], and to distinguish early from late segments of the distal tubule [220]. Since the dye has completely passed through all proximal tubules by the time the distal tubules are reached, distal tubules, filled with concentrated dye, stand out clearly (Figs. 6 and 7).

LG is neither secreted nor reabsorbed by the tubules [137], so it may be used to measure tubular fluid reabsorption in the same manner as inulin.

The advantage of LG is, of course, that water reabsorption can be followed in vivo from the increase in dye concentration. We have used LG dye for this purpose in split drop experiments [167]. LG could also be used to measure fluid reabsorption in continuous microperfusion experiments. As discussed above, care must be taken that the dye has been suitably purified, otherwise, contaminants may decrease sodium and water reabsorption. Also, LG V is better than LG SF, because unlike the latter it does not form a colorless compound with proteins and its extinction is pH insensitive.

LG is highly soluble in water and nontoxic; for these reasons, many investigators prefer this dye. It has been used for staining fluid for intratubular pressure measurements by the Landis method [39, 150, 153], for testing for leaks in recollection experiments [2], for more accurate determination of in vivo tubule diameters [40, 161], for visual control in microperfusion and microinjection experiments [13, 111, 113, 152, 186], and for determining loop passage times by intratubular dye injection [149]. LG has no effect on renal ultrastructure [114].

LG dye has been used to demonstrate an increase in tubular permeability in acute failure induced by mercuric chloride [11, 174] or by temporary ischemia [47]. Bank *et al.* [11] first reported that in mercury induced acute renal failure in rats, the dye concentration decreased as fluid moved along the proximal tubules. We have confirmed his passage time findings [174] and, in addition, showed that LG dye and inulin leave the tubules when injected intraluminally. These results suggest an increase in tubular permeability in acute renal failure. However, Oken and colleagues [54, 188] do not believe that tubular leakiness plays a significant role in acute renal failure.

Although the renal medulla will not be discussed, it should be mentioned that LG has been used for visualizing vasa recta, Henle's loops, and collecting tubules in the golden hamster and rat renal papilla in vivo [121, 161, 162–164], and for observing the excretion of protein casts by the collecting tubules [161, 164].

IV. Observations on Tubular Reabsorption

The reabsorption of fluid by the kidney tubules in vivo can be visualized with the incident light microscope using any of the following techniques:

(1) proximal occlusion time (collapse time) method,

(2) split-drop (split oil droplet; shrinking drop) method, and

(3) increase in intratubular concentration of a nonreabsorbed dye.

The first two methods have recently been discussed by Gottschalk and by Gertz [127]. For this reason, we will not discuss these methods in detail, but will emphasize matters not considered by these authors.

Table 14. Proximal tubular occlusion times in rats

Occlusion time (seconds)	Condition	Reference
7.7 ± 0.53	Antidiuresis, kidney surface rinsed with mineral oil	Steinhausen [166]
56.5 ± 5.9	Antidiuresis, kidney surface rinsed with Tyrode	
12 ± 1.4	Antidiuresis	Thoenes *et al.* [190]
160 ± 16.8	KCN (local application)	
13.8 ± 0.35	Antidiuresis	Wahl *et al.* [197]
16.7 ± 1.98	Hypotension (105–90 mm Hg)	
22.6 ± 1.16	Hypotension (80–70 mm Hg)	
17.2	Antidiuresis	Bojesen and Leyssac [16]
20 (16–24)	Antidiuresis	Leyssac [98]
ca. 27	Angiotensin i.v. (0.1 μg kg)	Leyssac [99]
103 ± 16	Ureteral pressure 40 mm Hg, kidney surface rinsed with mineral oil	Steinhausen [166]
287 ± 71	Ureteral pressure 40 mm Hg, kidney surface rinsed with Tyrode	

Values are means ± SE.

A. Proximal Occlusion Time

With this method, the kidney surface is observed through the microscope while the aorta above the renal arteries is suddenly occluded by means of a clamp. The occlusion time is recorded as the time between the interruption of blood flow to the kidney and the complete collapse of proximal tubule lumens (cf. Fig. 3). Leyssac [98–102] suggested that the occlusion time is an index of proximal tubular fluid reabsorptive rate. For a given tubule lumen volume, the shorter the occlusion time, the faster the rate of tubular reabsorption. The method is not without problems; the main criticism is that interruption of blood flow to the kidneys almost certainly affects tubular reabsorption.

Table 14 summarizes proximal tubular occlusion time measurements in rats. Occlusion time was markedly prolonged by a) increased ureteral pressure (initial tubule volume is greatly increased) or by b) potassium cyanide (oxidative metabolism is inhibited). Such extended occlusion times are probably not valid measures of the tubular reabsorptive rate before the occlusion, because of the effects of prolonged ischemia. Table 14 also shows that rinsing the kidney surface with Tyrode solution, instead of mineral oil, increases the occlusion time.

Steinhausen [166] attempt to obtain more objective measurements of proximal occlusion time by photographing the kidney surface at 1–5 sec intervals during tubular collapse. Under antidiuretic control conditions, the time for half of the proximal volume to be reabsorbed averaged 5.0 ± 0.42 SE sec ($n = 8$). Photography of the kidney during tubular collapse is, however, extremely difficult. When the aorta is clamped, the whole kidney rapidly shrinks. At the high magnifications necessary to accurately measure tubule diameter, it is hard to keep the tubule in focus. Also, optical contrast in the exsanguinated kidney is poor. Tubular lumens may be made more visible by measuring the occlusion time during the proximal passage of i.v. injected lissamine green.

B. Split-Drop Method

The split-drop method for studying proximal fluid absorption was introduced by Gertz [61]. The technique involves injecting a small quantity of aqueous perfusion fluid (usually isotonic sodium chloride solution) into a tubule previously filled with dyed castor oil. As the fluid is reabsorbed, the oil droplets come together. The shrinking of the aqueous droplet is photographed at precisely timed intervals. The reabsorptive half-time is the time for half of the tubular volume to be reabsorbed. For a given tubular volume, half-time is inversely related to tubular reabsorptive capacity.

Table 15 reviews split-drop measurements from the literature. The half-time for reabsorption from a saline droplet is normally about 10 seconds. The half-time is increased by adrenalectomy, massive isotonic saline loading, acute hypertension, partial renal venous occlusion, increased peritubular K^+, increased luminal Ca^{+2}, furosemide, mercury poisoning, or cyanide. The half-time is decreased by volume depletion.

Although the split-drop method is rather simple, there are many potential sources of error, which leads to difficulty in interpretation and conflict. Györy [74] suggested some approaches for standardizing the method. Nakajima *et al.* [123] and Gottschalk [127] believe that the method is of extremely limited value; their papers should be consulted for discussion of problems and pitfalls. Despite criticism, the method continues to be used. In two recent studies in the rat [70, 134], the question of the nature of fluid movement across the proximal tubule epithelium was examined. Persson *et al.* [134] concluded that as much as 30% of net fluid reabsorption was due to hydrostatic and oncotic forces. Green *et al.* [70] disagree and conclude that fluid reabsorption is almost exclusively coupled to solute reabsorption (mainly active sodium transport). The conclusion that pressure differences normally account for a large fraction of net fluid reabsorption [70] appears tenuous. In the split-drop experiment, the tubule is greatly distended [166] and intratubular hydrostatic pressure is elevated [134]. This may increase fluid movement through intercellular channels.

Table 15. Half-times from split drop experiments on proximal convoluted tubules in rats

Half-time (sec)	Test solution	Condition	Reference
6.4 ±0.4	Isotonic NaCl	Volume depleted	Weiner *et al.* [205]
9.0 ±0.8	Isotonic NaCl	Control	
8.5 ±0.24	Isotonic NaCl	Control, salt-free diet	Hayslett *et al.* [77]
8.7 ±0.24	Isotonic NaCl	Control, salt-rich diet	
11.9 ±0.42	Isotonic NaCl	Saline infusion (10% of body weight in 60 min)	
8.5 ±0.3	Isotonic NaCl	Control	Koch *et al.* [89]
14.3 ±0.7	Isotonic NaCl	Acute hypertension	
8.6 ±0.7	Isotonic NaCl	Control	Hierholzer *et al.* [85]
16.6 ±0.7	Isotonic NaCl	Adrenalectomy	
8.68 ±0.27	Isotonic NaCl	Control	Giebisch *et al.* [65]
8.92 ±0.40	Isotonic NaCl + 5% albumin	Control	
8.8 ±0.3	Isotonic NaCl	Adrenalectomy + cortisone	Hierholzer and Stolte [83]
9.5 ±0.4	Isotonic NaCl	Adrenalectomy + aldosterone	
17.0 ±0.8	Isotonic NaCl	Adrenalectomy + dexamethasone	
8.8 ±1.9	Isotonic NaCl	Diabetes insipidus	Gertz *et al.* [62]
9.8 ±0.84	Isotonic NaCl	Control	
8.9 ±0.9	Tubular fluid	Control	Heller and Nováková [80]
9.1 ±1.3	Isotonic NaCl	Control	
14.8 ±1.5	Isotonic NaCl	Isotonic saline, 0.5 ml/min for 60 min	
9.0 ±0.4	Isotonic NaCl	Control	Fülgraff and Heidenreich [57]
12.5 ±0.6	134 mEq/l Na^+, 20 mEq/l Ca^{++}, 154 mEq/l Cl^-	Control	
9.2 ±0.4	Isotonic NaCl	Control	Weinstein [207]
9.6 ±0.5	Isotonic NaCl + 10 mM glucose	Control	
13.6 ±0.7	300 mM mannitol + 1 mM 2,4-DNP	Control	
20.0 ±1.2	300 mM mannitol	Control	
20.3 ±1.4	Isotonic NaCl + 0.1 mM KCN	Control	
9.62 ±0.08	Isotonic NaCl or tubular fluid	Saline, 0.3 ml/min for 5 min	Heller [78]
10.23 ±0.81	Isotonic NaCl or tubular fluid	Control	

Table 15 (continued)

Half-time (sec)	Test solution	Condition	Reference
9.7 ±0.58	Isotonic NaCl	Control	Malnic *et al.* [110]
16.3 ±0.87	Isotonic NaCl	Furosemide	
9.7 ±0.5	Isotonic NaCl	Control	Spitzer and Windhager [159]
9.8 ±0.4	Isotonic NaCl	Control	Lewy and Windhager [97]
17.1 ±1.6	Isotonic NaCl	Partial renal venous occlusion	
10.0 ±0.55	Isotonic NaCl	Control	Landwehr *et al.* [93]
16.4 ±0.81	Isotonic NaCl	10% body wt. saline	
10.4 ±0.3	Isotonic NaCl	Ureteral pressure 40 mm Hg	Brenner *et al.* [29]
10.6 ±0.3	Isotonic NaCl	Control	
15.5 ±0.4	Isotonic NaCl	Aortic constriction (with reduction in GFR)	
11.0 ±1.56	Isotonic NaCl	Control	Steinhausen [166]
12.0 ±0.69	Tubular fluid	Control	
13.7 ±0.57	Tubular fluid	Ureteral pressure 40 mm Hg	
15.1 ±1.4	Isotonic NaCl	Ureteral pressure 40 mm Hg	
11.0 ±0.3	Isotonic NaCl	Control	Bank *et al.* [10]
12.5 ±0.37	150 mM Na^+, 143 mM Cl^-, 1.5 mM Ca^{++}, 10 mM acetate	Control	György [74]
13.5		Rats 20 days old	Čapek *et al.* [32]
16.9 ±1.24	115 mM NaCl, 25 mM $NaHCO_3$, 10 mM KCl, 2.5 mM $CaCl_2$	Peritubular capillaries perfused with 10 mM K^+	Brandis *et al.* [19]
16.9 ±4.2	Isotonic NaCl	Intoxication with sublimate	Steinhausen *et al.* [174]
8	Isotonic NaCl	Control	Wiederholt *et al.* [212]
38	Isotonic NaCl + 1 mM KCN	Control	
180	Isotonic NaCl + 10 mM KCN	Control	

Values are means ±SE. "Control" data are from nondiuretic (antidiuretic) rats.

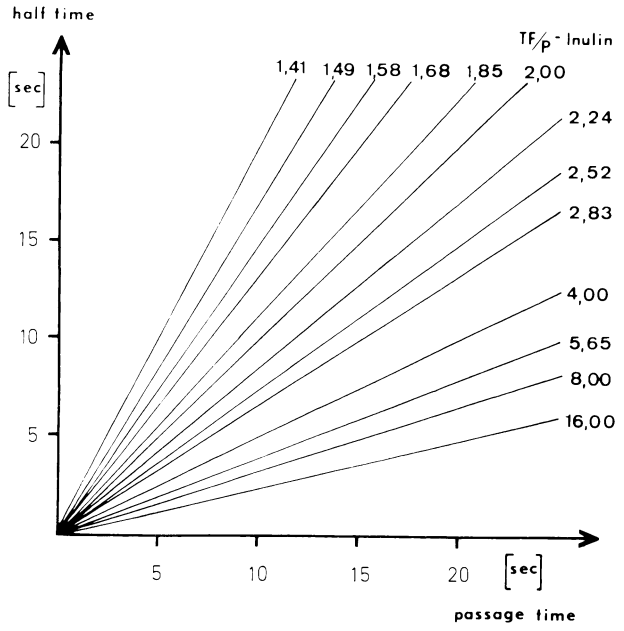

Fig. 10. Calculated end proximal TF/P inulin concentration ratios for corresponding reabsorptive half-times and proximal passage times. See text

C. Increase in Concentration of Nonreabsorbed Dyes

Tubular fluid reabsorption can be made visible by following the progressive concentration of nonreabsorbed dyes, such as LG [167, 174]. Using a microspectrophotometer, the increase in dye concentration may be quantitated. We found that there was good agreement between fluid reabsorption determined by this method and simultaneously measured from the decrease in solvent volume in a split-drop experiment. The method cannot be used to follow fluid reabsorption if the tubules are leaky to LG, as occurs in mercury poisoned [174] or ischemia-damaged [47] kidneys.

D. Relationship between Reabsorptive Half-Time and Passage Time

Proximal fractional fluid reabsorption may be determined either by a) micropuncture and measurement of the tubule fluid-to-plasma inulin concentration ratio (TF/P inulin) or b) measurement of reabsorptive half-time and passage time. The reabsorptive half-time, determined in an occlusion time experiment or in a split-drop experiment, gives the time required for 50% of the fluid volume to be reabsorbed. The passage time gives the time of exposure of tubular fluid to the proximal tubule epithelium. For example, if half-time is 10 sec and passage time is 10 sec, then the tubule will reabsorb 50% of the fluid volume presented, and a TF/P inulin ratio of 2

would be expected at the end of the proximal convoluted tubule. Figure 10 shows the TF/P inulin ratios expected for different combinations of reabsorptive half-time and passage time. The general relation is:

$$\text{TF/P inulin} = 2^{\text{passage time/half time}}$$

It is interesting to compare measured TF/P inulin ratios with results from passage time and reabsorptive half-time measurements. TF/P inulin ratios at the end of the accessible proximal tubule are about 3 at most in the nondiuretic rat (110, 215). For a passage time of 10.7 sec (see Table 7), a reabsorptive half-time of about 7 sec would be predicted from Figure 10. This is close to the 5 sec half-time measured with the proximal occlusion time method [166]. The reabsorptive half-time measured with the split-drop technique is about 10 sec (Table 15). This determination is, however, problematic, because the tubule lumen diameter is nearly twice normal [166]. The majority of studies [4, 8, 20, 98, 144, 151, 166] now indicate that proximal reabsorption does not depend on tubule diameter, so a 10 sec half-time in a tubule of double normal diameter would be equivalent to a 2.5 sec half-time in a tubule of normal diameter. These calculations suggest that estimates of fractional fluid reabsorption from these different approaches are in only rough agreement.

V. The Vascular Flow Bed

The blood vessel supply of a cortical nephron was described earlier (see p. 7). Afferent and efferent glomerular arterioles are generally thought to be the major sites of resistance to blood flow through the kidneys. The ratio of the resistances of these two vessels influences the glomerular capillary hydrostatic pressure. Resistance is a power function of vessel radius, so small changes in caliber will have a profound effect on renal blood flow and glomerular filtration rate. Afferent arterioles are not visible at the

Table 16. Length and inner diameters of blood vessels in the outer cortex of the rat

		Series 1 with F. Ullrich, 1975 (μ)	Series 2 with M. Abel, 1976 (μ)
Length	Afferent arteriole	186.0 ± 15.0 (45)	141.3 ± 17.4 (32)
	Efferent arteriole	224.0 ± 34.5 (41)	199.1 ± 12.3 (63)
Diameter	Interlobular artery	13.1 ± 0.8 (12)	—
	Afferent arteriole	8.3 ± 0.4 (12)	8.4 ± 0.4 (42)
	Efferent arteriole	6.8 ± 0.3 (12)	6.0 ± 0,2 (63)

Values are means ± SE (number of measurements).

Table 17. Vessel diameters, blood flow velocities, and blood flow rates in welling points and peritubular capillaries (vessel sections 1, 2, and 3) on the surface of the rat kidney cortex. Data are from control nondiuretic animals and animals 3 days after 1 hr renal artery occlusion (temporary ischemia). Means ± SE. (From Steinhausen *et al.* [171])

Vessel section	Diameter (microns)	Flow velocity (mm/sec)	Flow rate (nl/min)	Number of		
				Animals	Vessel sections	Measurements
Controls						
Welling point	23.00 ± 1.73 ↕ **	4.11 ± 0.59[b] ↕ *	102.53 ± 14.74[a] ↕ ***	9	12	12[c]
Vessel section No. 1	15.91 ± 0.92	2.32 ± 0.24 ↕ *	28.80 ± 4.14 ↕ *	9	27	133[d]
Vessel section No. 2	14.48 ± 0.64 ↕ *	1.61 ± 0.20	16.62 ± 1.14	6	10	53[d]
Vessel section No. 3	12.78 ± 0.25	1.51 ± 0.26	11.64 ± 2.16	4	7	20[d]
After temporary ischemia						
Welling point	20.17 ± 2.68	3.69 ± 0.67[b] ↕ *	70.77 ± 12.81[a] ↕ **	7	9	9[c]
Vessel section No. 1	15.07 ± 0.81	1.74 ± 0.20	20.22 ± 3.66	7	22	137[d]

[a] Calculated by multiplication of flow rate in vessel section No. 1 times degrees of ramification.
[b] Calculated from flow rate in vessel section No. 1 and diameter of the welling point.
[c] Vessel diameter.
[d] Flow velocity.

* $P < 0.05$ ** $P < 0.01$ *** $P < 0.001$.

surface of the rat kidney, and only the branching point of the efferent arteriole (welling point) can be seen. For this reason, we estimated the diameters of these vessels in fixed tissue. Together with F. Ullrich and M. Abel, we prepared vessel casts by in vivo perfusion with isotonic, isohydric, fixation fluids at normal arterial blood pressure. We found that such perfusions did not alter vessel diameters in the rat mesentery or on the kidney cortex surface. We cannot be positive, however, that vessel calibers inside the kidney were unaltered by perfusion and fixation. Table 16 summarizes our results for blood vessels in the outer cortex of the normal rat kidney. The arterioles appear to be quite narrow. Furthermore, afferent arterioles are wider than efferent arterioles. We and others [104, 158] have not found shunts between afferent and efferent arterioles in the outer cortex of the normal rat kidney.

Peritubular capillary blood flow is of particular interest in renal physiology because tubular fluid reabsorption depends on the uptake of reabsorbate by the capillaries surrounding the tubules [23–25, 97, 217]. We can

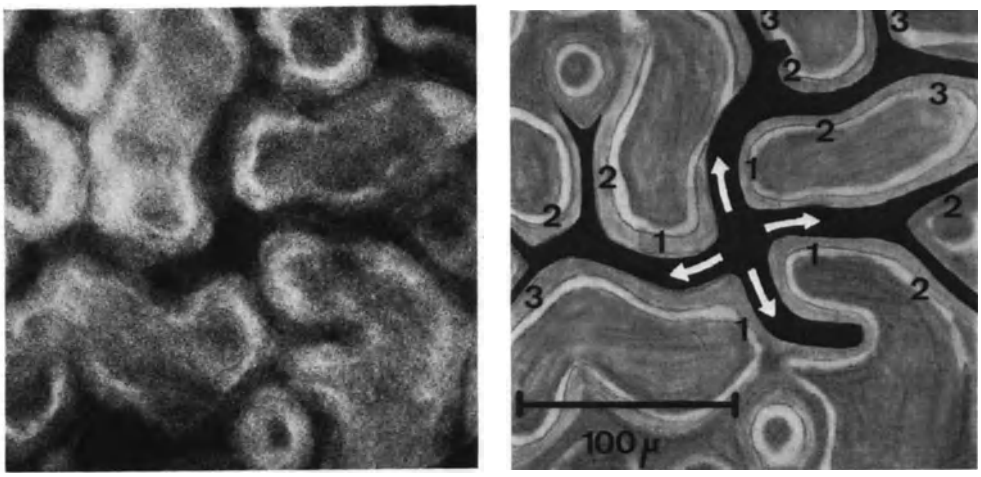

Fig. 11. Left: In vivo microphotograph of tubules and peritubular capillaries on the kidney surface of a male rat weighing 300 grams. The almost circular welling point is seen in the center of the picture. In vivo, it is recognizable from its intense red color. Right: Drawing based on the microphotograph on the left. The order of peritubular capillaries branching out from the welling point is numbered, and the flow direction is indicated. (From Steinhausen *et al.* [171])

easily observe the flow of blood in the peritubular capillaries on the surface of the exposed rat kidney cortex. However, quantitating the blood flow is difficult. We have measured capillary blood flow on the kidney cortex surface by high speed cinematography [171].

Table 17 summarizes data used in the calculation of peritubular capillary blood flow. The welling point gives rise to a branching system of peritubular capillaries designated, in order of branching, as "vessel section 1", "vessel section 2", etc. (see Fig. 11). Linear flow velocities in each vessel section were measured by high speed cinematography. From the linear velocity (in mm/sec) and vessel diameter (in microns), the corresponding blood flow rate (in nl/min) was calculated. The blood flow rate in the welling point was calculated by multiplying the number of first order vessel sections by the corresponding blood flow rate. We found that the welling point divides into an average of 3.56 ± 0.19 SE (9 animals) first order capillaries, and that the average blood flow rate per capillary was 28.8 nl/min. This gives a welling point blood flow rate of 103 nl/min. In cast preparations we have observed vessels branching off from the efferent arterioles before the welling point only rarely. Thus, the welling point blood flow may be equated with the efferent arteriolar blood flow.

The bottom part of Table 17 shows similar calculations of blood flow rate 3 days after 1 hr left renal artery occlusion. Such temporary ischemia produces severe acute failure of the damaged kidney. Blood flow rate was

decreased by 25 % below control. This modest reduction in blood flow cannot account for the reduction in inulin clearance to nearly zero.

In the normal kidney, the above estimate of efferent arteriolar blood flow agrees with values based on whole kidney measurements. If we multiply the blood flow in a single efferent arteriole (103 nl/min) by the number of such vessels or nephrons in both rat kidneys (65,600 according to Ref. [162]), divide by animal weight, and add the glomerular filtration rate measured with inulin in our experiments (8.5 ml/min-kg body weight–2 kidneys), we calculate a total kidney blood flow of 33 ml/min-kg body weight–2 kidneys. The corresponding values obtained in these same experiments, based on the PAH clearance or measurement of renal venous outflow, are 34 and 31 ml/min-kg body weight–2 kidneys, respectively. Thus, the three different methods are in remarkably good agreement. It must be noted, however, that blood flow in the kidney is not uniform, so it is not quite correct to extrapolate superficial cortical blood flow to the whole kidney. Wallin *et al.* [200] found that in the normal hydropenic rat, blood flow to superficial cortex is high, and that there is a progressive decrease from superficial to deep cortex.

Brenner *et al.* [22, 27] have estimated efferent arteriolar blood flow of single superficial cortical nephrons using two other approaches. They first attempted to collect blood quantitatively by micropuncture of the welling point. Later, they calculated efferent arteriolar blood flow from the single nephron glomerular filtration rate (inulin clearance), filtration fraction, and hematocrit. The filtration fraction was determined by measuring welling point and arterial plasma protein concentrations. With the first method, in Sprague-Dawley rats, they obtained an average efferent arteriolar blood flow of 152 nl/min. With the second method, in Munich-Wistar rats, they obtained a value of 114 nl/min. These values are somewhat higher than our determinations. A criticism of their approach is that insertion of a micropipette into the welling point may disturb the blood flow. When a quantitative collection of blood flow is attempted by the first method, the low resistance of the suction capillary may cause a spuriously high blood flow.

VI. Relationship Between Vascular and Tubular Systems (Cortical Countercurrent System)

If we look at the surface of the rat kidney cortex, we see what appears to be an irregular array of blood capillaries and tubular loops. In early studies using the lissamine green passage time method, Gertz *et al.* [63] and Steinhausen *et al.* [176] noticed that late proximal convoluted tubule loops were clustered together in the region of the welling point. Since the peritubular capillary network branches out from the welling point, and urine flows in the proximal tubule from early to late loops, we have counter-

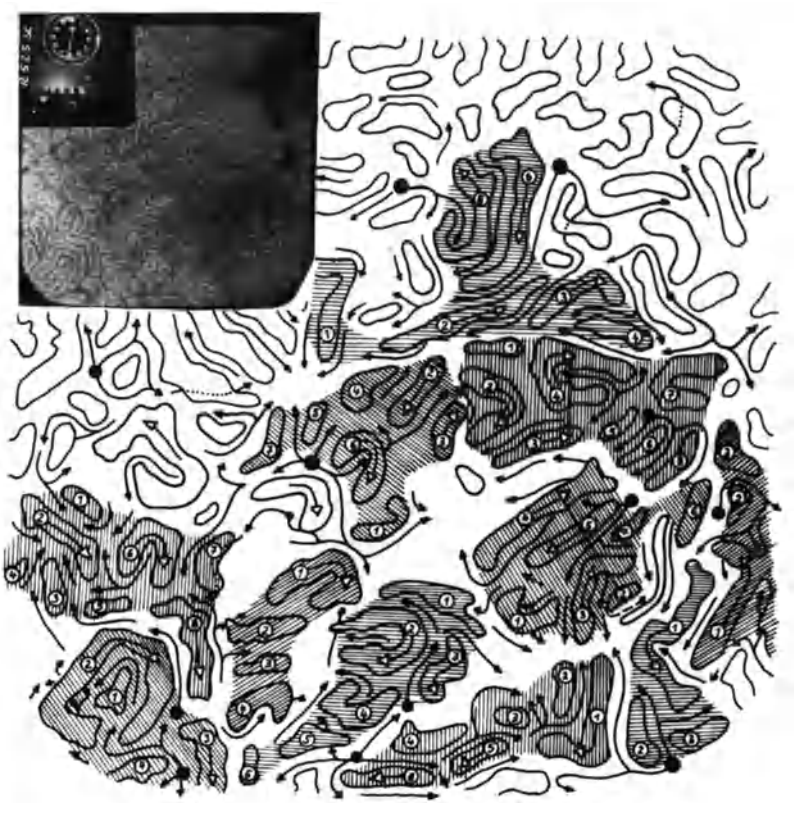

Fig. 12. Schematic drawing of the renal cortex surface of a rat, with the corresponding photomicrograph shown as an inset in the upper left hand corner. Black centers: Welling points. Black arrows: Peritubular capillaries and their flow direction. Hatched areas: Different nephrons. White arrows: Flow direction of tubular fluid. Numbers: Sequence of proximal tubular loops starting from the glomerulus. (From Steinhausen *et al.* [173])

current flow of blood and tubular urine on the surface of the rat kidney cortex. This cortical countercurrent system must not be confused with the medullary countercurrent systems involved in the osmotic concentration of the urine [219].

Several lines of evidence support the existence of a countercurrent system in the superficial cortex of the rat.

Anatomically, we find that each proximal convoluted tubule is preferentially supplied with blood from its own efferent arteriole, i.e. from its own welling point [172, 173]. This was demonstrated by preparing casts of nephrons and associated blood vessels (Fig. 1). Faarup *et al.* [49, 50] have confirmed this arrangement by histological methods.

The order of proximal loops (from early to late) was determined by following the passage of lissamine green in individual nephrons, and loop

position in relation to welling point was recorded [172, 173]. There was a highly significant ($P < 0.01$) inverse correlation between order of proximal loops and distance from the welling point. Figure 12 shows early proximal loops (low numbers) at a distance from the welling point and late proximal loops (high numbers) near the welling point.

The direction of blood flow in individual capillaries and in adjacent proximal tubular loops was assessed. Tubular fluid flow directions were determined with lissamine green, and blood flow directions were determined by observing the movement of blood cells. Figure 12 illustrates flow directions in a single microscopic field. We found that capillary blood flow was countercurrent to urine flow in 72.5% of 131 observations, in the same direction in 10.5%, and indeterminate in 17.0% [172, 173]. These results indicate that countercurrent flow predominates, but is not always present.

Although we find a preferential blood supply of each proximal convoluted tubule from its own welling point in the rat, there are numerous anastomoses between the capillaries of adjacent nephrons. This is easily demonstrated by microperfusion of a welling point. Depending on the perfusion rate, a large area of the most varied nephrons is perfused [9, 159]. A few surface loops of a nephron may normally be supplied from other welling points.

In the dog, there appears to be a close association between the efferent capillary network and proximal tubule of the same glomerulus only in the superficial (subcapsular) cortex [14]. In the bulk of the cortex, proximal tubules are dissociated from the efferent vessels of the same glomerulus, and are supplied by blood which has traversed other glomeruli. We have seen by in vivo microscopy that there is a cortical countercurrent system on the surface of the dog, pig, and rhesus monkey kidney (unpublished observations).

The functional significance of the cortical countercurrent system is still being investigated. Some aspects will be discussed below.

First, whether countercurrent flow is present primarily on the kidney surface or is present through the whole cortex is not known. It is clear, however, that it exists on the kidney surface, and thus the nephrons that are most often studied by micropuncture have this arrangement. Thus, it is relevant at least to in vivo micropuncture studies of cortical nephron function.

Second, an important area of current research is glomerular-tubular balance (see Gertz in Ref. [127]). Since each superficial proximal convoluted tubule is supplied primarily by its own efferent arteriole, and since peritubular capillary oncotic and hydrostatic pressures are important in tubular reabsorption, the close association between tubule and peritubular capillary blood supply permits glomerular-tubular balance to exist on a single nephron level.

Third, cortical countercurrent flow may influence secretory processes in the kidney. With fluorescent dyes, we have demonstrated that there is a preferential accumulation of dye in the late proximal loops around the welling point [168, 177]. The countercurrent arrangement may facilitate the transport of substances across the proximal tubule by decreasing the concentration difference between tubular fluid and peritubular blood.

Fourth, measurements with an oxygen electrode [130] demonstrate that oxygen tensions are higher in the late proximal loops (around the welling point) than in early proximal loops (distant from the welling point). Active transport processes along the proximal convoluted tubule may be affected by different local oxygen tensions.

Finally, Schulz *et al.* [154] suggested that cortical countercurrent flow may lead to errors in blood flow determinations with the ^{85}Kr washout method.

VII. Observations on Tubular Secretion

The renal handling of organic acid dyes played an important role in the early history of renal physiology [136]. In the last century, Heidenhain, on the basis of his studies with the sulfonic acid dye indigo carmine, claimed that tubular secretion played the primary role in urine formation. He observed this dye in the tubular cells, but could not find it in glomeruli. His views were opposed by Ludwig, who believed the kidney to be primarily a filtering-reabsorbing organ. Credit for proving the existence of tubular secretion is due to E. K. Marshall, Jr. In 1923, Marshall and Vickers [112a] obtained convincing evidence that phenolsulfonphthalein (phenol red) must be secreted by the dog kidney. They demonstrated that if arterial blood pressure was decreased to below 40 mm Hg (so as to abolish glomerular filtration), dye still accumulated in proximal tubules of the kidney cortex. Phenol red secretion by proximal tubules has been demonstrated in a number of in vitro and in vivo preparations (see Ref. [136 and 210] for review). The dye, however, is difficult to observe in the mammalian kidney in vivo, because it contrasts poorly with the renal surface. Also, its pK_A (7.8) is such that its color (red in alkaline solution, yellow in acid solution) is very pH sensitive in the physiological pH range. Kinter [87a] has studied the kinetics of dye transport in flounder kidney tubules in vitro, using a microspectrophotometer and chlorphenol red (pK_A 6.0). This dye is red at pH values above 6.7, so more reliable measurements of luminal concentrations can be made.

For the in vivo observation of dye secretion in the rat kidney, Steinhausen *et al.* [176a] used the fluorescent dye sulfonefluorescein. The structure of this dye differs from that of phenol red by a single oxygen bridge. Small amounts of sulfonefluorescein, injected intravenously, appear first round late proximal loops, in the vicinity of the welling point. The dye

concentration gradient between early and late proximal loops is readily determined with a microspectrophotometer. With low plasma concentrations of dye, this concentration gradient is maximal. The gradient probably reflects in part the fact that the late proximal loops are first supplied with dye rich blood from the welling point. If the plasma concentration of dye is increased, the secretory mechanism in the late proximal loops becomes saturated, and dye reaches the early (glomerular-near) proximal loops. The early-late proximal concentration gradient is then reduced. Rollhäuser [144a] has interpreted his studies on phenol red secretion in the rat kidney in a similar way. It is also possible that the concentration gradient observed reflects a higher secretory activity in the late proximal tubule. Finally, the dye gradient is increased by water reabsorption along the length of the tubule.

Probenecid, a well-known inhibitor of organic acid secretion, causes inhibition of sulfonefluorescein secretion. This inhibition is demonstrated by a significant reduction in the early-late proximal tubule concentration gradient, as well as a decrease in the sulfonefluorescein clearance. This general approach may be useful in studying the kinetics of dye transport in the mammalian kidney in vivo.

VIII. Conclusion

In this monograph, a survey was made of the methods and results of in vivo microscopic investigations of the kidney cortex. We have emphasized the approaches which we have personally tested. These methods have helped us to understand the relations between renal structure and function. Particular attention was given to data from the rat, since this animal has been most widely used in renal micropuncture studies. However, the extension of micropuncture techniques to other mammalian species will provide new insights. We considered the measurement of tubular diameters, tubular passage times, and tubular reabsorption. The peritubular capillary blood flow and the relations between blood flow and tubular urine were also discussed.

In vivo microscopy of the kidney provides a fascinating opportunity to study functional processes in the living animal, and to relate these observations to anatomy. This approach has a certain directness, which is lacking with many physiological measurements. Even so, we should be aware, in using the microscope, that what we think we see may not always be real or essential. To quote Goethe: "Was ist das Schwerste von allem? Was Dir das leichteste dünkt, mit den Augen zu sehen, was vor den Augen Dir liegt!"[3]

[3] "What is most difficult thing of all? The thing which seems easiest to you, to see with your eyes what lies in front of your eyes!"

References

1. Anagnostopoulos, T., Kinney, M. J., Windhager, E. E.: Salt and water reabsorption by short loops of Henle during renal vein constriction. Amer. J. Physiol. **220**, 1060–1066 (1971).
2. Andreucci, V. E., Herrera-Acosta, J., Rector, F. C., Jr., Seldin, D. W.: Measurement of single-nephron glomerular filtration rate by micropuncture: analysis of error. Amer. J. Physiol. **221**, 1551–1559 (1971).
3. Armsen, T., Schad, H., Reinhardt, H. W.: Die Harnstoffkonzentrierung in der Niere. II. Mikropunktionsexperimente an Ratten. Pflügers Arch. **313**, 222–244 (1969).
4. Arrizurieta-Muchnik, E.E., Lassiter, W. E., Lipham, E. M., Gottschalk, C. W.: Micropuncture study of glomerulotubular balance in the rat kidney. Nephron **6**, 418–436 (1969).
5. Bahlmann, J., Giebisch, G., Ochwadt, B., Schoeppe, W.: Micropuncture study of isolated perfused rat kidney. Amer. J. Physiol. **212**, 77–82 (1967).
6. Baines, A. D., Baines, C. J., de Rouffignac, C.: Functional heterogeneity of nephrons. I. Intraluminal flow velocities. Pflügers Arch. **308**, 244–259 (1969).
7. Baines, A. D., Rouffignac, C. de: Functional heterogeneity of nephrons. II. Filtration rates, intraluminal flow velocities and fractional water reabsorption. Pflügers Arch. **308**, 260–276 (1969).
8. Baines, A. D., Gottschalk, C. W., Leyssac, P. P.: Proximal luminal volume and fluid reabsorption in the rat kidney. Acta physiol. scand. **74**, 440–452 (1968).
9. Bank, N., Aynedjian, H. S., Wada, T.: Effect of peritubular capillary perfusion rate on proximal sodium reabsorption. Kidney Int. **1**, 397–405 (1972).
10. Bank, N., Koch, K. M., Aynedjian, H. S., Aras, M.: Effect of changes in renal perfusion pressure on the suppression of proximal tubular sodium reabsorption due to saline loading. J. clin. Invest. **48**, 271–283 (1969).
11. Bank, N., Mutz, B. F., Aynedjian, H. S.: The role of "leakage" of tubular fluid in anuria due to mercury poisoning. J. clin. Invest. **46**, 695–704 (1967).
12. Baumann, K., Huang, K. C.: Micropuncture and microperfusion study of L-glucose secretion in rat kidney. Pflügers Arch. **305**, 155–166 (1969).
13. Baumann, K., Oelert, H., Rumrich, G., Ullrich, K. J.: Ist Inulin zur Messung des Glomerulumfiltrates beim Warmblüter geeignet? Pflügers Arch. ges. Physiol. **282**, 238–241 (1965).
14. Beeuwkes, R., III: Efferent vascular patterns and early vascular-tubular relations in the dog kidney. Amer. J. Physiol. **221**, 1361–1374 (1971).
15. Bello-Reuss, E., Colindres, R. E., Pastoriza-Mũnoz, E., Mueller, R. A., Gottschalk, C. W.: Effects of acute unilateral renal denervation in the rat. J. clin. Invest. **56**, 208–217 (1975).
16. Bojesen, E., Leyssac, P. P.: Proximal tubular reabsorption in the rat kidney as studied by the occlusion time and lissamine green transit time technique. Acta physiol. scand. **76**, 213–235 (1969).

16a. Bonvalet, J. P., Champion, M., Wanstok, F., Berjal, G.: Absolute values of superficial and juxtamedullary single nephron glomerular filtration rate in unanesthetized rats. Proc. 26th Int. Physiol. Congr. **11**, 59 (1974).

17. Bordier, B., Ornstein, L., Wedeen, R. P.: The intrarenal distribution of tritiated para-aminohippuric acid determined by a modified technique of section freeze-dry radioautography. J. Cell Biol. **46**, 518–532 (1970).
18. Brackenridge, C. J.: Factors affecting the uptake of lissamine green by serum proteins. J. clin. Path. **13**, 149–155 (1960).
19. Brandis, M., Keyes, J., Windhager, E. E.: Potassium-induced inhibition of proximal tubular fluid reabsorption in rats. Amer. J. Physiol. **222**, 421–427 (1972).

20. Brenner, B. M., Bennett, C. M., Berliner, R. W.: The relationship between glomerular filtration rate and sodium reabsorption by the proximal tubule of the rat nephron. J. clin. Invest. **47**, 1358–1374 (1968).
21. Brenner, B. M., Berliner, R. W.: Relationship between extracellular volume and fluid reabsorption by the rat nephron. Amer. J. Physiol. **217**, 6–12 (1969).
22. Brenner, B. M., Daugharty, T. M., Ueki, I. F., Troy, J. L.: Quantitative assessment of proximal tubule function in single nephrons of the rat kidney. Amer. J. Physiol. **220**, 2058–2067 (1971).
23. Brenner, B. M., Falchuk, K. H., Keimowitz, R. I., Berliner, R. W.: The relationship between peritubular capillary protein concentration and fluid reabsorption by the renal proximal tubule. J. clin. Invest. **48**, 1519–1531 (1969).
24. Brenner, B. M., Galla, J. H.: Influence of postglomerular hematocrit and protein concentration on rat nephron fluid transfer. Amer. J. Physiol. **220**, 148–161 (1971).
25. Brenner, B. M., Troy, J. L.: Postglomerular vascular protein concentration: Evidence for a causal role in governing fluid reabsorption and glomerulotubular balance by the renal proximal tubule. J. clin. Invest. **50**, 336–349 (1971).
26. Brenner, B. M., Troy, J. L., Daugharty, T. M.: The dynamics of glomerular ultrafiltration in the rat. J. clin. Invest. **50**, 1776–1780 (1971).
27. Brenner, B. M., Troy, J. L., Daugharty, T. M., Deen, W. M., Robertson, C. R.: Dynamics of glomerular ultrafiltration in the rat. II. Plasma-flow dependence of GFR. Amer. J. Physiol. **223**, 1184–1190 (1972).
28. Brod, J.: The Kidney. London: Butterworths 1973.
29. Brunner, F. P., Rector, F. C., Jr., Seldin, D. W.: Mechanism of glomerulotubular balance. II. Regulation of proximal tubular reabsorption by tubular volume, as studied by stopped-flow microperfusion. J. clin Invest. **45**, 603–611 (1966).
30. Buentig, W. E., Earley, L. E.: Demonstration of independent roles of proximal tubular reabsorption and intratubular load in the phenomenon of glomerulotubular balance during aortic constriction in the rat. J. clin. Invest. **50**, 77–89 (1971).
31. Burwell, R. G.: Changes in the proximal tubule of the rabbit kidney after temporary complete renal ischemia. J. Path. Bact. **70**, 387–399 (1955).
32. Čapek, K., Dlouhă, H., Kraus, M.: Die Ansprechbarkeit der lokalen Reabsorptionskapazität im proximalen Konvolut der jungen Rattenniere. Pflügers Arch. **307**, R 61–62 (1969).
33. Čapek, K., Fernandez, J., Dlouhă, H.: Natriumresorption im proximalen Konvolut der jungen Rattenniere. Pflügers Arch. ges. Physiol. **300**, R 24 (1968).
34. Carrasquer, G., Wilczewski, T. W.: Effect of ureteral stop flow on PAH in lumen and cortex homogenate in the rat kidney. Proc. Soc. Exp. Biol. Med. (N.Y.) **137**, 284–291 (1971).
35. Christensen, P., Fredriksen, O.: The effect of some lissamine greens on gall bladder fluid absorption and frog skin sodium transport in vitro. Pflügers Arch. **331**, 160–171 (1972).
36. Cortell, S., Davidman, M., Gennari, F. J., Schwartz, W. B.: Catheter size as a determinant of outflow resistance and intrarenal pressure. Amer. J. Physiol. **223**, 910–915 (1972).
37. Cortell, S., Gennari, F. J., Davidman, M., Bossert, W. H., Schwartz, W. B.: A definition of proximal and distal tubular compliance. J. clin. Invest. **52**, 2330–2339 (1973).
38. Dangerfield, W. G., Smith, E. B.: An investigation of serum lipids and lipoproteins by paper electrophoresis. J. clin. Path. **8**, 132–139 (1955).
39. Davidman, M., Lalone, R. C., Alexander, E. A., Levinsky, N. G.: Some micropuncture techniques in the rat. Amer. J. Physiol. **221**, 1110–1114 (1971).

40. Deetjen, P.: Mikropunktionsuntersuchungen zur Wirkung von Furosemid. Pflügers Arch. ges. Physiol. **284**, 184–190 (1965).
41. Deetjen, P., Boylan, J. W., Kramer, K.: Physiology of the kidney and of water balance. New York: Springer 1975.
42. Dieterich, H. J., Kriz, W.: Zum Problem der Fixierung des Nierenmarks. Licht- und elektronenmikroskopische Untersuchungen an der Aussenzone der Rattenniere. Acta anat. (Basel) **74**, 267–289 (1969).
43. Dirks, J. H., Seely, J. F.: Micropuncture and diuretics. Ann. Rev. Pharmacol. **9**, 73–84 (1969).
44. Discombe, G., Jones, R. F., Winstanley, D. P.: The estimation of γ-globulin. J. clin. Path. **7**, 106–109 (1954).
45. Dörge, A., Nagel, W.: Die Wirkung von Lissamingrün auf den Natriumtransport an der isolierten Bauchhaut von Rana temporaria. Pflügers Arch. **313**, 11–18 (1969).
46. Edwards, J. G., Marshall, E. K., Jr.: Microscopic observations of the living kidney after the injection of phenolsulphonephthalein. Amer. J. Physiol. **70**, 489–495 (1924).
47. Eisenbach, G. M., Steinhausen, M.: Micropuncture studies after temporary ischemia of rat kidneys. Pflügers Arch. **343**, 11–25 (1973).
48. Elmer, M., Leyssac, P. P.: A study of the effects of some chemically well-defined lissamine greens on tubular and overall renal function in the rat (with an evaluation of the validity of lissamine green transit time measurements in studies of tubular function). Acta physiol. scand. **87**, 296–306 (1973).
49. Faarup, P., Ryø, G., Saelan, H.: Selective capillary vascularization of the nephron in the rat kidney. Acta path. microbiol. scand. **80A**, 139–141 (1972).
50. Faarup, P., Saelan, H., Ryø, G.: Correlation between tubules and capillaries and size of interstitial space in the functioning rat kidney. Acta path. microbiol. scand. **79A**, 607–616 (1971).
51. Falchuk, K. H., Brenner, B. H., Tadokoro, M., Berliner, R. W.: Oncotic and hydrostatic pressures in peritubular capillaries and fluid reabsorption by proximal tubule. Amer. J. Physiol. **220**, 1427–1433 (1971).
52. Fetterman, G. H., Fabrizio, N. S., Studnicki, F. M.: Microdissection of the nephron: The method and its applications. In: Laboratory diagnosis of kidney diseases, ed. by F. W. Sunderman and F. W. Sunderman, Jr. St. Louis: W. H. Green 1970.
53. Finberg, J. P. M., Peart, W. S.: Renal tubular flow dynamics during angiotensin diuresis in the rat. Brit. J. Pharmacol. **39**, 357–372 (1970)
54. Flamenbaum, W., McDonald, F. D., DiBona, G. F., Oken, D. E.: Micropuncture study of renal tubular factors in low dose mercury poisoning. Nephron **8**, 221–234 (1971).
54a. Frick, A: Proximal tubular reabsorption of inorganic phosphate during saline infusion in the rat. Amer. J. Physiol. **223**, 1034–1040 (1972).
55. Frohnert, P. P., Höhmann, B., Zwiebel, R., Baumann, K.: Free flow micropuncture studies of glucose transport in the rat nephron. Pflügers Arch. **315**, 66–85 (1970).
56. Frömter, E., Hegel, U.: Transtubuläre Potentialdifferenzen an proximalen und distalen Tubuli der Rattenniere. Pflügers Arch. ges. Physiol. **291**, 107–120 (1966).
57. Fülgraff, G., Heidenreich, O.: Mikropunktionsuntersuchungen über die Wirkung von Calciumionen auf die Resorptionskapazität und auf die prozentuale Resorption im proximalen Konvolut von Ratten. Naunyn-Schmiedebergs Arch. Pharmak. exp. Path. **258**, 440–451 (1967).
58. Fülgraff, G., Heidenreich, O., Heintze, K., Osswald, H.: Die Wirkung von α- und β-Sympathomimetica und Sympatholytica auf die renale Exkretion und Resorption von Flüssigkeit und Elektrolyten in Ausscheidungs- und Mikropunktionsversuchen an Ratten. Naunyn-Schmiedebergs Arch. Pharmak. exp. Path. **262**, 295–308 (1969).

59. Fülgraff, G., Meiforth, A.: Effects of prostaglandin E_2 on excretion and reabsorption of sodium and fluid in rat kidneys (micropuncture studies). Pflügers Arch. **330**, 243–256 (1971).
60. Galaske, R., Galaske, W., Steinhausen, M.: Beeinflussen Passagezeit-Bestimmungen die renale Natrium-Ausscheidung der Ratte? Pflügers Arch. **319**, R 78 (1970).
61. Gertz, K.H.: Transtubuläre Natriumchloridflüsse und Permeabilität für Nichtelektrolyte im proximalen und distalen Konvolut der Rattenniere. Pflügers Arch. ges. Physiol. **276**, 336–356 (1963).
62. Gertz, K. H., Kennedy, G. C., Ullrich, K. J.: Mikropunktionsuntersuchungen über die Flüssigkeitsrückresorption aus den einzelnen Tubulusabschnitten bei Wasserdiurese (Diabetes insipidus). Pflügers Arch. ges. Physiol. **278**, 513–519 (1964).
63. Gertz, K. H., Mangos, J. A., Braun, G., Pagel, H. D.: On the glomerular tubular balance in the rat kidney. Pflügers Arch. ges. Physiol. **285**, 360–372 (1965).
64. Ghiron, M.: Über eine neue Methode mikroskopischer Untersuchung am lebenden Organismus. Zbl. Physiol. **26**, 613–617 (1912).
65. Giebisch, G., Klose, R. M., Malnic, G., Sullivan, W. J., Windhager, E. E.: Sodium movement across single perfused proximal tubules of rat kidneys. J. Gen. Physiol. **47**, 1175–1194 (1964).
66. Gilmore, J. P.: Renal physiology. Baltimore: Williams & Wilkins 1972.
67. Goldacre, R. J., Sylven, B.: A rapid method for studying tumor blood supply using systemic dyes. Nature (Lond.) **184**, 63–64 (1959).
68. Gottschalk, C. W., Mylle, M.: Micropuncture study of pressures in proximal tubules and peritubular capillaries of the rat kidney and their relation to ureteral and renal venous pressures. Amer. J. Physiol. **185**, 430–439 (1956).
69. Gottschalk, C. W., Mylle, M.: Micropuncture study of pressures in proximal and distal tubules and peritubular capillaries of the rat kidney during osmotic diuresis. Amer. J. Physiol. **189**, 323–328 (1957).
70. Green, R., Windhager, E. E., Giebisch, G.: Protein oncotic pressure effects on proximal tubular fluid movement in the rat. Amer. J. Physiol. **226**, 265–276 (1974).
71. Greven, J., Fülgraff, G.: Probleme bei der Bestimmung der prozentualen Resorption aus Halbwertzeit und Passagezeit von proximalen Tubuli von Rattennieren. Pflügers Arch. **315**, 38–44 (1970).
72. Griffith, L. D., Bulger, R. E., Trump, B. F.: The ultrastructure of the functioning kidney. Lab. Invest. **16**, 220–246 (1967).
72a. Gross, F., Möhring, J.: Renal pharmalogy, with special emphasis on aldosteron and angiotensin. Ann. Rev. Pharm. **13**, 57–90 (1973).
73. Grossmann, D. F., Frey, J.: The renal clearance of lissamine green in the rat. In: Progress in nephrology, ed. by G. Peters and F. Roch-Ramel. Berlin-Heidelberg-New York: Springer 1969.
74. Györy, A. Z.: Reexamination of the split oil droplet method as applied to kidney tubules. Pflügers Arch. **324**, 328–343 (1971).
74a. Hanssen, O. E.: The relationship between glomerular filtration and length of the proximal convoluted tubules in mice. Acta path. microbiol. scand. **53**, 265–279 (1961).
75. Harris, C. A., Baer, P. G., Chirito, E., Dirks, J. H.: Composition of mammalian glomerular filtrate. Amer. J. Physiol. **227**, 972–976 (1974).
76. Hartman, M. E.: Direct visualization of glomeruli in the immature mouse. Amer. J. Physiol. **180**, 163–166 (1955).
77. Hayslett, J. P., Kashgarian, M., Epstein, F. H.: Changes in proximal and distal tubular reabsorption produced by rapid expansion of extracellular fluid. J. clin. Invest. **46**, 1254–1263 (1967).

78. Heller, J.: Micropuncture study of the mechanism of natriuresis after a short infusion of isotonic saline in rats. Physiol. bohemoslov. **20**, 139–145 (1971).
79. Heller, J.: The influence of lissamine green on tubular reabsorption of electrolytes and water in rats. Pflügers Arch. **323**, 27–33 (1971).
80. Heller, J., Nováková, A.: Time course of changes of some renal parameters during infusion of isotonic saline solution in rats. Physiol. bohemoslov. **17**, 355–367 (1968).
81. Heller, J., Nováková, A.: Proximal tubular reabsorption during renal vasodilation and increased arterial blood pressure in saline loaded rats. Pflügers Arch. **309**, 250–265 (1969).
82. Henry, L. N., Lane, C. E., Kashgarian, M.: Micropuncture studies of the pathophysiology of acute renal failure in the rat. Lab. Invest. **19**, 309–314 (1968).
83. Hierholzer, K., Stolte, H.: The proximal and distal tubular action of adrenal steroids on Na reabsorption. Nephron **6**, 188–204 (1969).
84. Hierholzer, K., Ullrich, K. J.: Grundzüge der Nierenphysiologie. In: Handbuch der experimentellen Pharmakologie, Vol. 24, ed. by H. Herken, p. 1–61. Berlin-Heidelberg-New York: Springer 1969.
85. Hierholzer, K., Wiederholt, M., Stolte, H.: Hemmung der Natriumresorption im proximalen und distalen Konvolut adrenalektomierter Ratten. Pflügers Arch. ges. Physiol. **291**, 43–62 (1966).
86. Holmberg, B.: On the permeability to lissamine green and other dyes in the course of cell injury and cell death. Exp. Cell Res. **22**, 406–414 (1961).
87. Joppich, R., Deetjen, P.: The relation between the reabsorption of urea and of water in the distal tubule of the rat kidney. Pflügers Arch. **329**, 172–185 (1971).
87a. Kinter, W. B.: Chlorphenol red influx and efflux: microspectrophotometry of flounder kidney tubules. Amer. J. Physiol. **211**, 1152–1164 (1966).
88. Knox, F. G., Wright, F. S., Howards, S. S., Berliner, R. W.: Effect of furosemide on sodium reabsorption by proximal tubule of the dog. Amer. J. Physiol. **217**, 192–198 (1969).
89. Koch, K. M., Aynedjian, H. S., Bank, N.: Effect of acute hypertension on sodium reabsorption by the proximal tubule. J. clin. Invest. **47**, 1696–1709 (1968).
90. Krause, H. H., Dume, Th., Koch, K. M., Ochwadt, B.: Intratubulärer Druck, glomerulärer Capillardruck und Glomerulumfiltrat nach Furosemid und Hydrochlorothiazid. Pflügers Arch. ges. Physiol. **295**, 80–89 (1967).
91. Kriz, W.: Histophysiologische Untersuchungen an der Rattenniere bei Sublimatvergiftung. Z. Zellforsch. **57**, 914–952 (1962).
92. Kriz, W., Dieterich, H. J.: Das Lymphgefäss-system der Niere bei einigen Säugetieren. Licht- und elektronenmikroskopische Untersuchungen. Z. Anat. Entwickl.-Gesch. **131**, 111–147 (1970).
93. Landwehr, D. M., Klose, R. M., Giebisch, G.: Renal tubular sodium and water reabsorption in the isotonic sodium chloride-loaded rat. Amer. J. Physiol. **212**, 1327–1333 (1967).
94. Langer, K. H., Thoenes, W., Wiederholt, M.: Licht- und elektronenmikroskopische Untersuchungen am proximalen Tubuluskonvolut der Rattenniere nach intraluminaler Ölinjektion. Pflügers Arch. **302**, 149–165 (1968).
95. Lassiter, W. E.: Kidney. Ann. Rev. Physiol. **37**, 371–393 (1975).
96. Levine, D. Z., Liebau, G., Fischbach, H., Thurau, K.: Micropuncture studies on the dog kidney. II. Reabsorptive characteristics of the proximal tubule during spontaneous and experimental variations in GFR and during drug induced natriuresis. Pflügers Arch. **304**, 365–375 (1968).
97. Lewy, J. E., Windhager, E. E.: Peritubular control of proximal tubular fluid reabsorption in the rat kidney. Amer. J. Physiol. **214**, 943–954 (1968).

98. Leyssac, P. P.: Dependence of glomerular filtration rate on proximal tubular reabsorption of salt. Acta physiol. scand. **58**, 236–242 (1963).
99. Leyssac, P. P.: The in vivo effect of angiotensin on the proximal tubular reabsorption of salt in rat kidneys. Acta physiol. scand. **62**, 436–448 (1964).
100. Leyssac, P. P.: The luminal occlusion time of proximal tubules in kidneys of young rats. Acta physiol. scand. **64**, 176–181 (1965).
101. Leyssac, P. P.: The regulation of proximal tubular reabsorption in the mammalian kidney. Acta physiol. scand. **70**, Suppl. 291, 11–151 (1966).
102. Leyssac, P. P.: Renal salt and water excretion in different states of an intrarenal control system. Proc. Roy. Soc. Med. **62**, 1111–1116 (1969).
103. Liebau, G., Levine, D. Z., Thurau, K.: Micropuncture studies on the dog kidney I. The response of the proximal tubule to changes in systemic blood pressure within and below the autoregulatory range. Pflügers Arch. **304**, 57–68 (1968).
104. Ljungqvist, A., Wägermark, J.: The adrenergic innervation of intrarenal glomerular and extra-glomerular circulatory routes. Nephron **7**, 218–229 (1970).
105. Lockhart, E. A., Dirks, J. H., Carrière, S.: Effects of triflocin on renal tubular reabsorption and blood flow distribution. Amer. J. Physiol. **223**, 89–96 (1972).
106. Lowitz, H. D., Stumpe, K. O., Ochwadt, B.: Natrium- und Wasserresorption in den verschiedenen Abschnitten des Nephrons beim experimentellen renalen Hochdruck der Ratte. Pflügers Arch. **304**, 322–335 (1968).
107. Lowitz, H. D., Stumpe, K. O., Ochwadt, B.: Mikropunktionsuntersuchungen der geklammerten Niere bei einseitig nephrektomierten Ratten mit experimentellem renalen Hochdruck. Pflügers Arch. **309**, 212–223 (1969).
108. Lynch, R. E., Schneider, E. G., Strandhoy, J. W., Willis, L. R., Knox, F. G.: Effect of lissamine green dye on renal sodium reabsorption in the dog. J. Appl. Physiol. **35**, 169–171 (1973).
109. Maddox, D. A., Deen, W. M., Brenner, B. M.: Dynamics of glomerular ultrafiltration: VI. Studies in the primate. Kidney Int. **5**, 271–278 (1974).
110. Malnic, G., Enokibara, H., Mello Aires, M., Vieira, F. L.: Die Wirkung von Furosemid und NaCl-Belastung auf die Chloridausscheidung im Einzelnephron der Rattenniere. Pflügers Arch. **309**, 21–37 (1969).
111. Malnic, G., Giebisch, G.: Some electrical properties of distal tubular epithelium in the rat. Amer. J. Physiol. **223**, 797–808 (1972).
111a. Malvin, R. L., Fusco, M. M.: Renal function in unanesthetized normal and diabetes insipidus rats. J. Appl. Physiol. **22**, 380–382 (1967).
112. Mályusz, M., Mendoza-Osorio, V., Ochwadt, B.: Nierenfunktion bei Ratten mit experimentellem DOCA-Hochdruck. Pflügers Arch. **332**, 28–39 (1972).
112a. Marshall, E. K., Jr., Vickers, J. L.: The mechanism of the elimination of phenolsulphonephthalein by the kidney; a proof of secretion by the convoluted tubules. Bull. Johns Hopk. Hosp. **34**, 1–7 (1923).
113. Maude, D. L., Scott, W. N., Shehadeh, I., Solomon, A. K.: Further studies on the behavior of inulin and serum albumin in rat kidney tubule. Pflügers Arch. ges. Physiol. **285**, 313–316 (1965).
114. Maunsbach, A. B.: Absorption of I^{125}-labeled homologous albumin by rat kidney proximal tubule cells. J. Ultrastruct. Res. **15**, 197–241 (1966).
115. Maunsbach, A. B.: The influence of different fixatives and fixation methods on the ultrastructure of rat kidney proximal tubule cells. J. Ultrastruct. Res. **15**, 242–282 (1966).
116. Maunsbach, A. B.: Observations on the segmentation of the proximal tubule in the rat kidney. Comparison of results from phase contrast, fluorescence, and electron microscopy. J. Ultrastruct. Res. **16**, 239–258 (1966).

117. Maunsbach, A. B., Madden, S. C., Latta, H.: Variations in fine structure of renal tubular epithelium under different condition of fixation. J. Ultrastruct. Res. **6**, 511–530 (1962).
118. Meng, K.: Mikropunktionsuntersuchungen über die saluretische Wirkung von Hydrochlorothiazid, Acetazolamid und Furosemid. Naunyn-Schmiedebergs Arch. exp. Path. Pharmak. **257**, 355–371 (1967).
119. Morel, F., Murayama, Y.: Simultaneous measurement of unidirectional and net sodium fluxes in microperfused rat proximal tubules. Pflügers Arch. **320**, 1–23 (1970).
120. Morel, F., Rouffignac, C. de: Kidney. Ann. Rev. Physiol. **35**, 17–54 (1973).
121. Morgan, T., Berliner, R. W.: Permeability of the loop of Henle, vasa recta and collecting duct to water, urea and sodium. Amer. J. Physiol. **215**, 108–115 (1968).
122. Müller, H.: Über die Entstehung von UV-Stasen in den Kapillaren der Froschschwimmhaut. Z. Biol. **113**, 9–38 (1961).
123. Nakajima, K., Clapp, J. R., Robinson, R. R.: Limitations of the shrinking-drop micropuncture technique. Amer. J. Physiol. **219**, 345–357 (1970).
124. Netter, H.: Theoretische Biochemie. Physikalisch-chemische Grundlagen der Lebensvorgänge. Berlin-Göttingen-Heidelberg: Springer 1959.
125. Oelert, H., Baumann, K., Gekle, D.: Permeabilitätsmessungen einiger schwacher organischer Säuren aus dem distalen Konvolut der Rattenniere. Pflügers Arch. **307**, 178–189 (1969).
126. Oliver, J.: Nephrons and kidneys. New York: Hoeber 1968
127. Orloff, J., Berliner, R. W., Editors: Handbook of Physiology, Sect. 8: Renal physiology. Washington, D. C.: American Physiological Society 1973.
128. Orloff, J., Burg, M.: Kidney. Ann. Rev. Physiol. **33**, 83–130, (1971).
129. Ott, C. E., Navar, L. G., Guyton, A. C.: Pressures in static and dynamic states from capsules implanted in the kidney. Amer. J. Physiol. **221**, 394–400 (1971).
130. Parekh, N., Ehrlich, J., Steinhausen, M.: Pattern of oxygen tension in the renal surface of rats. Proc. 26th Int. Physiol. Congr. **11**, 343 (1974).
131. Parekh, N., Popa, G., Galaske, R., Galaske, W., Steinhausen, M.: Renal test dyes. I. Physical and chemical properties of some dyes suitable for renal passage time measurements. Pflügers Arch. **343**, 1–9 (1973).
131a. Parekh, N., Popa, G., Steinhausen, M.: Renal test dyes. III. Effect of dyes suitable for renal passage time measurements on renal function. Pflügers Arch. ges. Physiol. Physiol. **364**, 77–81 (1976).
132. Pease, D. C.: Electron microscopy of the vascular bed of the kidney cortex. Anat. Rec. **121**, 701–721 (1955).
133. Pease, D. C.: Electron microscopy of the tubular cells of the kidney cortex. Anat. Rec. **121**, 723–743 (1955).
134. Persson, A. E. G., Ågerup, B., Schnermann, J.: The effect of luminal application of colloids on rat proximal tubular net fluid flux. Kidney Int. **2**, 203–213 (1972).
135. Peter, K.: Untersuchungen über Bau und Entwicklung der Niere. Jena: Gustav Fischer 1927.
136. Pitts, R. F.: Physiology of the kidney and body fluids, 3rd ed. Chicago: Year Book Medical Publishers 1974.
137. Popa, G., Parekh, N., Steinhausen, M.: Renal test dyes. II. Renal handling of dyes suitable for renal passage time measurements. Pflügers Arch. **350**, 273–280 (1974).
138. Rector, F. C., Jr., Brunner, F. P., Seldin, D. W.: Mechanism of glomerulotubular balance. I. Effect of aortic constriction and elevated ureteropelvic pressure on glomerular filtration rate, fractional reabsorption, transit time, and tubular size in the proximal tubule of the rat. J. clin. Invest. **45**, 590–602 (1966).

139. Rector, F. C., Jr., Martinez-Maldonado, M., Kurtzman, N. A., Sellman, J. C., Oerther, F., Seldin, D. W.: Demonstration of a hormonal inhibitor of proximal tubular reabsorption during expansion of extracellular volume with isotonic saline. J. clin. Invest. **47**, 761–773 (1968).
140. Rennick, B. R.: Renal excretion of drugs: Tubular transport and metabolism. Ann. Rev. Pharmacol. **12**, 141–156 (1972).
141. Roch-Ramel, F., Chométy, F., Peters, G.: Urea concentrations in tubular fluid and in renal tissue of nondiuretic rats. Amer. J. Physiol. **215**, 429–438 (1968).
142. Roch-Ramel, F., Diézi, J., Chométy, F., Michoud, P., Peters, G.: Disposal of large urea overloads by the rat kidney: a micropuncture study. Amer. J. Physiol. **218**, 1524–1532 (1970).
143. Roch-Ramel, F., Jotterand, N.: Natriuretic effect of lissamine green. Experientia (Basel) **26**, 683 (1970).
144. Rodicio, J., Herrera-Acosta, J., Sellman, J. C., Rector, F. C., Jr., Seldin, D. W.: Studies on glomerulotubular balance during aortic constriction, ureteral obstruction and venous occlusion in hydropenic and saline-loaded rats. Nephron **6**, 437–456 (1969).
144a. Rollhäuser, H.: Untersuchungen über den örtlichen und zeitlichen Ablauf der Phenolrot-Ausscheidung in den Tubuli der unbeeinflußten Rattenniere. Z. Zellforsch. **51**, 348–355 (1960).
145. Rostgaard, J., Thuneberg, L.: Electron microscopical observations on the brush border of proximal tubule cells of mammalian kidney. Z. Zellforsch. **132**, 473–496 (1972).
146. Schneider, E. G., Dresser, T. P., Lynch, R. E., Knox, F. G.: Glomerulotubular balance in dogs with chronic salt retention. Nephron **8**, 46–56 (1971).
147. Schneider, E. G., Dresser, T. P., Lynch, R. E., Knox, F. G.: Sodium reabsorption by proximal tubule of dogs with experimental heart failure. Amer. J. Physiol. **220**, 952–957 (1971).
148. Schneider, E. G., Lynch, R. E., Willis, L. R., Knox, F. G.: Single-nephron filtration rate in the dog. Amer. J. Physiol. **222**, 667–673 (1972).
149. Schnermann, J.: Microperfusion study of single short loops of Henle in rat kidney. Pflügers Arch. ges. Physiol. **300**, 255–282 (1968).
150. Schnermann, J., Horster, M., Levine, D. Z.: The influence of sampling technique on the micropuncture determination of GFR and reabsorptive characteristics of single rat proximal tubules. Pflügers Arch. **309**, 48–58 (1969).
151. Schnermann, J., Levine, D. Z., Horster, M.: A direct evaluation of the Gertz hypothesis on single rat proximal tubules in vivo: Failure of the tubular volume to be
the sole determinant of the reabsorptive rate. Pflügers Arch. **308**, 149–165 (1969).
152. Schnermann, J., Wahl, M., Liebau, G., Fischbach, H.: Balance between tubular flow rate and net fluid reabsorption in the proximal convolution of the rat kidney. I. Dependency of reabsorptive net fluid flux upon proximal tubular surface area at spontaneous variations of filtration rate. Pflügers Arch. **304**, 90–103 (1968).
153. Schnermann, J., Wright, F. S., Davis, J. M., Stackelberg, W. v., Grill, G.: Regulation of superficial nephron filtration rate by tubulo-glomerular feedback. Pflügers Arch. **318**, 147–175 (1970).
154. Schulz, V., Schwarz, W., Hutten, H.: Vergleichende Durchblutungsmessungen an der Rattenniere zur Reproduzierbarkeit von Kr-85-Auswaschkurven. Pflügers Arch. **312**, 206–219 (1969).
155. Schweizer, H. R.: Künstliche organische Farbstoffe und ihre Zwischenprodukte. Berlin-Göttingen-Heidelberg-New York: Springer 1964.

156. Solomon, S.: Pressure and flow in proximal tubules of rat kidneys. Experientia (Basel) **18**, 37 (1962).
157. Sperber, I.: Studies on the mammalian kidney. Zool. Bidrag Uppsala **22**, 249–432 (1944).
158. Spinelli, F. R., Wirz, H., Brücher, Ch., Pehling, G.: Nonexistence of shunts between afferent and efferent arterioles of juxtamedullary glomeruli in dog and rat kidneys. Nephron **9**, 123–128 (1972).
159. Spitzer, A., Windhager, E. E.: Effect of peritubular oncotic pressure changes on proximal tubular fluid reabsorption. Amer. J. Physiol. **218**, 1188–1193 (1970).
160. Steinhausen, M.: Eine Methode zur Differenzierung proximaler und distaler Tubuli der Nierenrinde von Ratten in vivo und ihre Anwendung zur Bestimmung tubulärer Strömungsgeschwindigkeiten. Pflügers Arch. ges. Physiol. **277**, 23–35 (1963).
161. Steinhausen, M.: In vivo-Beobachtungen an der Nierenpapille von Goldhamstern nach intravenöser Lissamingrün-Injektion. Pflügers Arch. ges. Physiol. **279**, 195–213 (1964).
162. Steinhausen, M.: Der tubuläre Harnstrom (dargestellt unter besonderer Berücksichtigung intravitalmikroskopischer Untersuchungen an Ratten-, Katzen- und Goldhamsternieren). Habil.-Schrift, Heidelberg 1965.
163. Steinhausen, M.: Mikrozirkulation von Lissamingrün in der Warmblüterniere. Film D 886 and accompanying publication. Inst. wiss. Film, Göttingen 1965/1966.
164. Steinhausen, M.: Ausscheidung von Eiweisszylindern durch das Sammelrohrsystem des Goldhamsters. In: Aktuelle Probleme der Nephrologie. Berlin-Heidelberg-New York: Springer 1966.
165. Steinhausen, M.: Dextran und tubulärer Harnstrom. In: Genese und Therapie des hämorrhagischen Schocks. Stuttgart: Georg Thieme 1966.
166. Steinhausen, M.: Messungen des tubulären Harnstromes und der tubulären Reabsorption unter erhöhtem Ureterdruck. Intravitalmikroskopische Untersuchungen an der Nierenrinde von Ratten. Pflügers Arch. ges. Physiol. **298**, 105–130 (1967).
167. Steinhausen, M.: Tubuläre Resorption an der Nierenoberfläche der Ratte (Split drop). Film E 1680 and accompanying publication. Inst. wiss. Film, Göttingen 1971/1972.
168. Steinhausen, M.: Further information on the cortical countercurrent system in rat kidney. Yale J. Biol. Med. **45**, 451–456 (1972).
169. Steinhausen, M.: Physiologie. Eine Einführung in das Basiswissen. Stuttgart: W. Kohlhammer 1975.
170. Steinhausen, M., Eisenbach, G. M.: Glomeruläre Filtration und Mikrozirkulation der Rattenniere. Film E 1679 T and accompanying publication. Inst. wiss. Film, Göttingen 1971/1972.
171. Steinhausen, M., Eisenbach, G. M., Böttcher, W.: High-frequency microcinematographic measurements on peritubular blood flow under control conditions and after temporary ischemia of rat kidneys. Pflügers Arch. ges. Physiol. **339**, 273–288 (1973)
172. Steinhausen, M., Eisenbach, G. M., Galaske, R.: Counter-current system in the renal cortex of rats. Science **167**, 1631–1633 (1970).
173. Steinhausen, M., Eisenbach, G. M., Galaske, R.: A counter-current system of the surface of the renal cortex of rats. Pflügers Arch. ges. Physiol. **318**, 244–258 (1970).
174. Steinhausen, M., Eisenbach, G. M., Helmstädter, V.: Concentration of lissamine green in proximal tubules of antidiuretic and mercury poisoned rats and the permeability of these tubules . Pflügers Arch. ges. Physiol. **311**, 1–15 (1969).

174a. Steinhausen, M., Hill, E., Parekh, N.: Intravital microscopical studies of the tubular urine flow in the conscious rat. Pflügers Arch. ges. Physiol. **362**, 261–264 (1976).
175. Steinhausen, M., Iravani, I., Schubert, G. E., Taugner, R.: Auflichtmikroskopie und Histologie der Tubulusdimensionen bei verschiedenen Diuresezuständen. Virchows Arch. path. Anat. **336**, 503–527 (1963).
176. Steinhausen, M., Loreth, A., Olson, S.: Messungen des tubulären Harnstromes, seine Beziehungen zum Blutdruck und zur Inulin-clearance. Intravitalmikroskopische Untersuchungen an der Nierenrinde von Ratten und Katzen. Pflügers Arch. ges. Physiol. **286**, 118–141 (1965).
176a. Steinhausen, M., Müller, P., Parekh, N.: Renal test dyes IV. Intravital fluorescence microscopy and microphotometry of the tubularly secreted dye sulfonefluorescein. Pflügers Arch. ges. Physiol. **364**, 83–89 (1976).
177. Steinhausen, M., Parekh, N., Popa, G.: Further studies on the cortical countercurrent system in the rat kidney. Pflügers Arch. ges. Physiol. **343**, R 94 (1973).
178. Steinhausen, M., Weidinger, H.: Durchblutungsänderung an der Nierenoberfläche unter Sympathikus-Reizung. Film E 1681 and accompanying publication. Inst. wiss. Film. Göttingen 1971/1972.
179. Steinhausen, M., Weidinger, H., Ross, H. J., Eisenbach, G. M.: Incident-light microscopy of the renal surface during stimulation of the sympathetic renal nerves. In: Progress in nephrology, ed. by G. Peters and F. Roch-Ramel. Berlin-Heidelberg-New York: Springer 1969.
180. Stolte, H., Wiederholt, M., Fuchs, G., Hierholzer, K.: Time course of development of transtubular sodium concentration differences in proximal surface tubules of the rat kidney. Pflügers Arch. ges. Physiol. **313**, 252–270 (1969).
181. Stumpe, K. O., Lowitz, H. D., Ochwadt, B.: Mikropunktionsuntersuchung am distalen Tubulus beim Goldblatt-Hochdruck der Ratte. Pflügers Arch. **304**, 336–350 (1968).
182. Stumpe, K. O., Lowitz, H. D., Ochwadt, B.: Function of juxtamedullary nephrons in normotensive and chronically hypertensive rats. Pflügers Arch. **313**, 43–52 (1969).
183. Stumpe, K. O., Lowitz, H. D., Ochwadt, B.: Beschleunigte Natriurese und Diurese beim Hochdruck: Folge einer Resorptionshemmung in der Henleschen Schleife. Pflügers Arch. **330**, 290–301 (1971).
184. Stumpe, K. O., Ochwadt, B.: Wirkungen von Aldosteron auf die Natrium- und Wasserresorption im proximalen Tubulus bei chronischer Kochsalzbelastung. Pflügers Arch. ges. Physiol. **300**, 148–160 (1968).
185. Suzuki, A.: Micropuncture study of distal tubular function of cat kidney. Jap. J. Pharmacol. **21**, 75–85 (1971).
186. Tanner, G. A., Klose, R. M.: Micropuncture study of inulin reabsorption in Necturus kidney. Amer. J. Physiol. **211**, 1036–1038 (1966).
187. Tanner, G. A., Selkurt, E. E.: Kidney function in the squirrel monkey before and after hemorrhagic hypotension. Amer. J. Physiol. **219**, 597–603 (1970).
188. Thiel, G., McDonald, F. D., Oken, D. E.: Micropuncture studies of the basis for protection of renin depleted rats from glycerol induced acute renal failure. Nephron **7**, 67–79 (1970).
189. Thoenes, W., Hierholzer, K., Wiederholt, M.: Gezielte Fixierung von Nierentubuli in vivo durch Mikroperfusion zur licht- und elektronenmikroskopischen Untersuchung. Klin. Wschr. **43**, 794–795 (1965).
190. Thoenes, W., Langer, K. H., Warning, A.: Funktionsmorphologische Studien zur energetischen Insuffizienz des Nierentubulus. Untersuchungen an der Rattenniere nach Oberflächenbetropfung mit Kaliumcyanid. Klin. Wschr. **46**, 696–708 (1968).

191. Thurau, K., Deetjen, P.: Kinematographische Untersuchungen am Warmblüternephron. Nachr. Akad. Wiss. Göttingen, Math. Phys. Kl. **H 2**, 27–37 (1961).
192. Tisher, C. C., Bulger, R. E., Valtin, H.: Morphology of renal medulla in water diuresis and vasopressin-induced antidiuresis. Amer. J. Physiol. **220**, 87–94 (1971).
193. Trendelenburg, W.: Der Gesichtssinn. Grundzüge der physiologischen Optik, 2nd edition. Berlin-Göttingen-Heidelberg: Springer 1961.
194. Valtin, H.: Renal function: Mechanisms preserving fluid and solute balance in health. Boston: Little, Brown 1973.
195. Van Liew, J. B., Deetjen, P., Boylan, J. W.: Glucose reabsorption in the rat kidney. Dependence on glomerular filtration. Pflügers Arch. ges. Physiol. **295**, 232–244 (1967).
196. Vieira, F. L., Malnic, G.: Hydrogen ion secretion by renal cortical tubules as studied by an antimony microelectrode. Amer. J. Physiol. **214**, 710–718 (1968).
197. Wahl, M., Liebau, G., Fischbach, H., Schnermann, J.: Balance between tubular flow rate and net fluid reabsorption in the proximal convolution of the rat kidney. II. Reabsorptive characteristics during constriction of the renal artery. Pflügers Arch. ges. Physiol. **304**, 297–314 (1968).
198. Wahl, M., Nagel, W., Fischbach, H., Thurau, K.: On the application of the occlusion time method for measurements of lateral net fluxes in the proximal convolution of the rat kidney. Pflügers Arch. ges. Physiol. **298**, 141–153 (1967).
199. Walker, A. M., Oliver, J.: Methods for the collection of fluid from single glomeruli and tubules of the mammalian kidney. Amer. J. Physiol. **134**, 562–579 (1941).
200. Wallin, J. D., Blantz, R. C., Katz, M. A., Andreucci, V. E., Rector, F. C., Jr., Seldin, D. W.: Effect of saline diuresis on intrarenal blood flow in the rat. Amer. J. Physiol. **221**, 1297–1304 (1971).
201. Walther, D., Lindemann, G.: Morphologische supravitale Veränderungen der Niere bei Diurese und Antidiurese. Virchows Arch. Abt. B **4**, 176–187 (1969).
202. Walther, D., Schoeppe, W.: Der Einfluß des intratubulären Druckes auf die Tubulusweite unter normalen und pathologischen Bedingungen. Klin. Wschr. **43**, 1092–1094 (1965).
203. Wardener, H. E. de: Control of sodium reabsorption. Brit med. J. **3**, 611–616, 676–683 (1969).
204. Weiner, I. M.: Excretion of drugs by the kidney. In: Handbook of Experimental Pharmacology, Vol. 28, No. 1, ed. by B. B. Brodie and J. R. Gillette, pp. 328–353. Berlin-Heidelberg-New York: Springer 1971.
205. Weiner, M. W., Weinman, E. J., Kashgarian, M., Hayslett, J. P.: Accelerated reabsorption in the proximal tubule produced by volume depletion. J. clin. Invest. **50**, 1379–1385 (1971).
206. Weinman, E. J., Kashgarian, M., Hayslett, J. P.: Role of peritubular protein concentration in sodium reabsorption. Amer. J. Physiol. **221**, 1521–1528 (1971).
207. Weinstein, S. W.: Proximal tubular energy metabolism, sodium transport, and permeability in the rat. Amer. J. Physiol. **219**, 978–981 (1970).
208. Weinstein, S. W., Klose, R. M.: Micropuncture studies on energy metabolism and sodium transport in the mammalian nephron. Amer. J. Physiol. **217**, 498–504 (1969).
209. Welling L. W., Grantham, J. J.: Physical properties of isolated perfused renal tubules and tubular basement membranes. J. clin. Invest. **51**, 1063–1075 (1972).
210. Wesson, L. G., Jr.: Physiology of the human kidney. New York: Grune & Stratton 1969.
211. Wiederholt, M., Hierholzer, K., Windhager, E. E., Giebisch, G.: Microperfusion study of fluid reabsorption in proximal tubules of rat kidney. Amer. J. Physiol. **213**, 809–818 (1967).

212. Wiederholt, M., Langer, K. H., Thoenes, W., Hierholzer, K.: Funktionelle und morphologische Untersuchungen am proximalen und distalen Konvolut der Rattenniere zur Methode der gespaltenen Ölsäule (Split-Oil Droplet Method). Pflügers Arch. ges. Physiol. **302**, 166–191 (1968).
213. Wiederholt, M., Stolte, H., Brecht, J. P., Hierholzer, K.: Mikropunktionsuntersuchungen über den Einfluß von Aldosteron, Cortison und Dexamethason auf die renale Natriumresorption adrenalektomierter Ratten. Pflügers Arch. ges. Physiol. **292**, 316–333 (1966).
214. Willis, L. R., Schneider, E. G., Lynch, R. E., Knox, F. G.: Effect of chronic alteration of sodium balance on reabsorption by proximal tubule of the dog. Amer. J. Physiol. **223**, 34–39 (1972).
215. Windhager, E. E.: Micropuncture techniques and nephron function. London: Butterworths 1968.
216. Windhager, E. E.: Kidney, water and electrolytes. Ann. Rev. Physiol. **31**, 117–172 (1969).
217. Windhager, E. E., Lewy, J. E., Spitzer, A.: Intrarenal control of proximal tubular reabsorption of sodium and water. Nephron **6**, 247–259 (1969).
218. Winkel, K. zum, Hallwachs, O., Steinhausen, M.: Kameraszintigraphie und Isotopennephrographie an der Hundeniere und deren Überprüfung durch die Intravitalmikroskopie. Fortschr. Röntgenstr. **108**, 382–393 (1968).
219. Wirz, H., Hargitay, B., Kuhn, W.: Lokalisation des Konzentrierungsprozesses in der Niere durch direkte Kryoskopie. Helv. physiol. pharmacol. Acta **9**, 196–207 (1951).
220. Wright, F. S.: Increasing magnitude of electrical potential along the renal distal tubule. Amer. J. Physiol. **220**, 624–638 (1971).
221. Wright, F. S., Giebisch, G.: Glomerular filtration in single nephrons. Kidney Int. **1**, 201–209 (1972).
222. Yarger, W. W., Aynedjian, H. S., Bank, N.: A micropuncture study of post-obstructive diuresis in the rat. J. clin. Invest. **51**, 625–637 (1972).

Sitzungsberichte der Heidelberger Akademie der Wissenschaften
Mathematisch-naturwissenschaftliche Klasse
Erschienene Jahrgänge

Inhalt des Jahrgangs 1966:

1. W. Rauh und I. Jäger-Zürn. Zur Kenntnis der Hydrostachyaceae. 1. Teil. DM 39.80.
2. M. R. Lemberg. Chemische Struktur und Reaktionsmechanismus der Cytochromoxydase (Atmungsferment). DM 12.00.
3. R. Berger. Differentiale höherer Ordnung und Körpererweiterungen bei Primzahlcharakteristik. (vergriffen).
4. E. Kauker. Die Tollwut in Mitteleuropa von 1953 bis 1966. (vergriffen).
5. Y. Reenpää. Axiomatische Darstellung des phänomenal-zentralnervösen Systems der sinnesphysiologischen Versuche Keidels und Mitarbeiter. DM 12.00.

Inhalt des Jahrgangs 1967/68:

1. E. Freitag. Modulformen zweiten Grades zum rationalen und Gaußschen Zahlkörper. (vergriffen).
2. H. Hirt. Der Differentialmodul eines lokalen Prinzipalrings über einem beliebigen Ring. (vergriffen).
3. H. E. Suess, H. D. Zeh und J. H. D. Jensen. Der Abbau schwerer Kerne bei hohen Temperaturen. DM 12.00.
4. H. Puchelt. Zur Geochemie des Bariums im exogenen Zyklus. (vergriffen).
5. W. Hückel. Die Entwicklung der Hypothese vom nichtklassischen Ion. DM 12.00.

Inhalt des Jahrgangs 1968:

1. A. Dinghas. Verzerrungssätze bei holomorphen Abbildungen von Hauptbereichen automorpher Gruppen mehrerer komplexer Veränderlicher in eine Kähler-Mannigfaltigkeit. DM 12.00.
2. R. Kiehl. Analytische Familien affinoider Algebren. DM 12.00.
3. R. Düren, G.-P. Raabe und Ch. Schlier. Genaue Potentialbestimmung aus Streumessungen: Alkali-Edelgas-Systeme. DM 12.00.
4. E. Rodenwaldt. Leon Battista Alberti — ein Hygieniker der Renaissance. DM 12.00.

Inhalt des Jahrgangs 1969/70:

1. N. Creutzburg und J. Papastamatiou. Die Ethia-Serie des südlichen Mittelkreta und ihre Ophiolithvorkommen. DM 25.60.
2. E. Jammers, M. Bielitz, I. Bender und W. Ebenhöh. Das Heidelberger Programm für die elektronische Datenverarbeitung in der musikwissenschaftlichen Byzantinistik. DM 12.00.
3. M. Knebusch. Grothendieck- und Wittringe von nichtausgearteten symmetrischen Bilinearformen. DM 23.—.
4. W. Rauh und K. Dittmar. Weitere Untersuchungen an Didiereaceen. 3. Teil. DM 44.20.
5. P. J. Beger. Über „Gurkörperchen" der menschlichen Lunge. DM 23.40.

Inhalt des Jahrgangs 1971:

1. E. Letterer. Morphologische Äquivalentbilder immunologischer Vorgänge im Organismus. (vergriffen).
2. J. Herzog und E. Kunz. Die Wertehalbgruppe eines lokalen Rings der Dimension 1. DM 19.50.
3. W. Maier. Aus dem Gebiet der Funktionalgleichungen. DM 12.00.
4. H. Hepp und H. Jensen. Klassische Feldtheorie der polarisierten Kathodenstrahlung und ihre Quantelung. DM 18.20.
5. H. Koppe und H. Jensen. Das Prinzip von d'Alembert in der Klassischen Mechanik und in der Quantentheorie. (vergriffen).
6. W. Doerr. Wandlungen der Krankheitsforschung. (vergriffen).
7. K. Hoppe. Über die spektrale Zerlegung der algebraischen Formen auf der Grassmann-Mannigfaltigkeit. DM 35.10.